Assignment of potential neurotransmitters and neuromodulators to physiologically and morphologically identified olfactory interneurons

Inaugural-Dissertation

zur Erlangung des Doktorgrades
der Mathematisch-Naturwissenschaftlichen Fakultät
der Universität zu Köln

vorgelegt von
Debora Fuscà
aus Saarbrücken
Köln 2012

Zoologisches Institut
Universität zu Köln

Berichterstatter: Prof. Dr. Peter Kloppenburg
Prof. Dr. Ansgar Büschges
Tag der mündlichen Prüfung: 13.11.2012

Contents

Abbreviations

ACh ..... acetylcholine
AL(s) ..... antennal lobe(s)
AST-A ..... allatostatins
AST-A-LIR . AST-A-like immunoreactivity
AST-A-lir ... AST-A-like immunoreactive
AT ..... allatotropin
AT-LIR ..... AT-like immunoreactivity
AT-lir ..... AT-like immunoreactive
CCAP ..... crustacean cardioactive peptide
ChAT ..... choline acetyltransferase
ChAT-LIR .. ChAT-like immunoreactivity
ChAT-lir .... ChAT-like immunoreactive
CLSM ..... confocal laser scanning microscope / microscopy
dChAT ..... *Drosophila* ChAT
DMSO ..... dimethyl sulfoxide
eFMRFa .... extended FMRFamides
EGTA ..... ethylene glycol bis(2-aminoethyl ether)-N,N,N′,N′-tetraacetic acid
FaRP ..... FMRFamide-related peptides
GABA ..... γ-aminobutyric acid
GABA-LIR .. GABA-like immunoreactivity
GABA-lir ... GABA-like immunoreactive
HEK ..... human embryonic kidney
HEPES ..... 4-(2-hydroxyethyl)-1-piperazineethanesulfonic acid
HRP ..... horse radish peroxidase

iACT ..... inner antennocerebral tract

LMS ..... myosuppressin

LN I ..... type I LN(s)

LN II(a/b) .. type II(a/b) LN(s)

LN(s) ..... local interneuron(s)

MALDI-TOF MS Matrix-assisted laser desorption/ionization-time of flight mass spectrometry

Mas-AT ..... *Manduca sexta* AT

MIP ..... myoinhibitory peptide

MIP-LIR .... MIP-like immunoreactivity

MIP-lir ..... MIP-like immunoreactive

MS ..... mass spectrometry

OSN(s) ..... olfactory sensory neuron(s)

PBS ..... phosphate buffered saline

PBS-TX ..... phosphate buffered saline containing Triton X-100

PBT ..... phosphate buffered saline containing Tween

PCC ..... Pearson's correlation coefficient

PDM ..... product of the difference from the mean

PN(s) ..... projection neuron(s)

RT ..... room temperature

SDS-PAGE .. sodium dodecyl sulfate polyacrylamide gel electrophoresis

sNPF ..... short neuropeptides F

TK ..... tachykinin

TKRP ..... tachykinin-related peptides

TKRP-LIR .. TKRP-like immunoreactivity

TKRP-lir .... TKRP-like immunoreactive

TTX ..... tetrodotoxin

uPN(s) ..... uniglomerular projection neuron(s)

VSG ..... ventrolateral soma group

Zusammenfassung

Verhaltens-, sowie physiologische Studien zeigen, dass die Verarbeitung von Geruchsinformationen durch neuronale Interaktionen in den Glomeruli des Antennallobus (AL) von Insekten bedingt wird. Diese Interaktionen werden von einem komplexen Netzwerk von hemmenden und erregenden lokalen Interneuronen (LNs) vermittelt, die das Abstimmungsprofil der Projektionsneurone reguliert und schließlich die Geruchsrepresentation formt. LNs haben speziefische morphologische und intrinsische elektrophysiologische Eigenschaften und können neben GABA und Acetylcholin unterschiedliche Peptide enthalten und ausschütten, die potentiell als Neurotransmitter oder -modulatoren agieren können. In *Periplaneta americana* sind zwei LN-Haupttypen bekannt: 1) Spikende Typ I LNs (LN I), die bei Duftstimulation Na^+-abhängige Aktionspotentiale generieren und GABA-immunreaktiv sind, und 2) nicht-spikende Typ II LNs (LN II), unterteilt in Typ IIa und Typ IIb, mit unbekanntem Transmitter, die keine Na^+-abhängige Aktionspotentiale generieren. Diese Diversität innerhalb der LN Population impliziert auch unterschiedliche Funktionen verschiedener LN Typen bei der olfaktorischen Informationsverarbeitung.

Während es bereits eine Reihe von Untersuchungen zur chemischen Organisation des AL verschiedener Insekten gibt, wurden hier die Transmitter- und Modulatorkandidaten direkt identifizierten LNs mit unterschiedlichen physiologischen Eigenschaften zugeordnet. Hierzu kombinierte ich "whole cell patch clamp" Aufnahmen, Einzelzellfärbungen und immuncytochemische Methoden.

Mittels eines Antikörpers gegen das biosynthetisierende Enzym Acetylcholintransferase (ChAT), welcher cholinerge Neurone markiert, konnte gezeigt werden, dass eine Untergruppe der nicht-spikenden LN IIa mit distinkten physiolo-

gischen und morphologischen Eigenschaften cholinerg ist. In diesen Typ IIa1 LNs (LN IIa1) rief eine Geruchsstimmulation Depolarisationen mit Ca^{2+}-getragene "Spikelets", aber keine Na^{+}-abhängige Aktionspotentiale hervor.
Im Zuge einer vollständigen Aufklärung der Botenstoffe der identifizierten LN-Typen wurde außerdem das Neuropeptid Allatotropin (AT) den spikenden LN I und Tachykinine (TKRPs) sowohl den LN I als auch den nicht-spikenden LN IIa1 zugeordnet. Dies legt nahe, dass in LN I AT zusammen mit GABA ausgeschüttet wird, wohingegen TKRPs sowohl in LN I zusammen mit GABA, als auch in LN IIa1 zusammen mit Acetylcholin ausgeschüttet werden.
Um einen möglichst vollständigen Informationensatz von individuellen, eindeutig identifizierten Neuronen erhalten zu können, wurde außerdem eine Methode etabliert, die es ermöglicht, Massenspektrometrie in elektrophysiologisch und morphologisch identifizierten Interneuronen durchzuführen.

Abstract

Behavioral and physiological studies show that processing of odor information involves neuronal interactions among the glomeruli in the insect antennal lobe (AL). These interactions are mediated by a complex network of inhibitory and excitatory local interneurons (LNs), that structures the olfactory representation and ultimately determines the tuning profile of projection neurons. LNs have distinct morphological and intrinsic electrophysiological properties and in addition to GABA and acetylcholine LNs may contain and release various peptides, that can potentially act as neurotransmitters or neuromodulators. In *Periplaneta americana* two main LN types are known: 1) Spiking type I LNs (LN I), that generate Na^+ driven action potentials upon odor stimulation and exhibit GABA-like immunoreactivity (GABA-LIR) and 2) nonspiking type II LNs, subdivided into type IIa and type IIb, with unknown transmitter, that do not generate Na^+ driven action potentials. This LN diversity implies that these neurons serve distinct functions in the olfactory system. Currently, the morphologically and physiologically distinct LN subtypes are not very well matched with the variety of neurotransmitters and -modulators. This, however, is an important prerequisite for a detailed understanding of the role of LNs in the olfactory circuit. While previous studies have investigated the neurochemical organization of the AL in various insect species, I unequivocally assigned the inventory of potentially neuroactive substances to the functionally distinct LN types.

For this purpose, I used a combination of whole-cell patch-clamp recording, single cell labeling and immunocytochemical methods, to analyze the inventory of neuroactive substances in the AL of *P. americana*. Using an antibody against the biosynthetic enzyme choline acetyltransferase (ChAT), a marker for cholin-

ergic neurons, a subset of the nonspiking LN IIa with distinct physiological and morphological properties was identified as cholinergic. In these type IIa1 LNs (LN IIa1), odor stimulation evoked depolarizations that generated Ca^{2+} driven 'spikelets', but not Na^{+} driven action potentials.

In an effort to form a complete messenger profiling of identified LN types, the neuropeptide allatotropin (AT) was assigned to spiking LN I and tachykinin-related peptides (TKRPs) were assigned to both LN I and nonspiking LN IIa1. This suggests, that AT is coreleased with GABA in LN I, while TKRPs are coreleased with GABA in LN I as well as with acetylcholine in LN IIa1.

Finally, a method is introduced, that offers the possibility to perform mass spectrometry in electrophysiologically and morphologically identified interneurons, which allows a comprehensive data set of individual neurons to be built up.

1 Introduction

The sense of smell is critically important for the survival of most species. The first-order olfactory systems of insects (antennal lobe) and vertebrates (olfactory bulb) share many features in structural organization and physiological function that are strikingly similar, suggesting similar mechanisms of olfactory information processing across phyla (Eisthen, 2002; Hildebrand & Shepherd, 1997; Strausfeld & Hildebrand, 1999; Wilson & Mainen, 2006). Due to the vast analogies, the insect antennal lobe (AL) successfully serves as a model to study general principles of signal processing on the network level, with the advantage of anatomical simplicity and a limited number of identified neurons involved in olfaction (Davis, 2004; Fiala, 2007; Laurent, 1999; Wilson & Laurent, 2005).
As an important step towards the goal to understand the role of the different neuronal components in the olfactory circuit in detail, I investigated the inventory of potentially neuroactive substances in subtypes of local interneurons in the cockroach AL.

1.1 The insect olfactory system

The insect antennal lobe (AL) is the first relay where synaptic processing of olfactory inputs occurs. (for review, see Boeckh & Tolbert, 1993; Galizia & Rössler, 2010; Vosshall & Stocker, 2007; Davis, 2004; Hildebrand & Shepherd, 1997; Strausfeld & Hildebrand, 1999; Wilson, 2008). The neuropil is subdivided into functional units called glomeruli, where the axons of olfactory sensory neurons (OSNs) form synapses onto uniglomerular projection neurons (uPNs) and local interneurons (LNs). OSNs expressing the same type of olfactory receptors converge into

the same glomerulus (Gao *et al.* , 2000). The uPNs carry the integrated olfactory information to higher order neuropils such as the mushroom bodies and the lateral lobe of the protocerebrum (illustrated in figure 1). Within the AL, LNs mediate complex excitatory and inhibitory interactions between the glomerular pathways to structure the olfactory representation, which ultimately determines the tuning profile of the projection (output) neurons (reviewed in Davis, 2004; Hildebrand & Shepherd, 1997; Strausfeld & Hildebrand, 1999; Vosshall & Stocker, 2007; Wilson, 2008; Wilson & Mainen, 2006; Bazenov *et al.* , 2001; Olsen *et al.* , 2007; Silbering *et al.* , 2008; Stopfer, 2005).

1.2 Local interneurons in olfactory information processing

Based on early immunocytochemical and electrophysiological work, local interneurons have historically been regarded as mostly GABAergic and inhibitory (Distler, 1989; Hoskins *et al.* , 1986; Christensen *et al.* , 1993; Waldrop *et al.* , 1987). During the last decade, however, immunocytochemical and mass spectrometrical studies on various insects made it increasingly clear that LNs are a much more heterogeneous population of neurons that, in addition to GABA, may also contain and release other potential neurotransmitters and neuromodulators. These include acetylcholine (ACh; Shang *et al.* , 2007), various peptides, biogenic amines (reviewed in Homberg, 1999a; Nassel & Homberg, 2006; Schachtner *et al.* , 2005), and amino acids such as glutamate (Daniels *et al.* , 2008). Moreover, LNs can have very different morphological and intrinsic electrophysiological properties (Olsen & Wilson, 2008; Chou *et al.* , 2010; Husch *et al.* , 2009a,b; Seki & Kanzaki, 2008; Seki *et al.* , 2010).

In *P. americana* two main LN types have been described: Spiking type I LNs (LN I), that generate Na^+ driven action potentials upon depolarizing current injection or odor stimulation and exhibit GABA-like immunoreactivity (GABA-LIR) and non-spiking type II LNs (LN II) with unknown transmitter content. The latter lack

voltage dependent Na^+ channels and thus, do not generate Na^+ driven action potentials. Nonspiking LN II can be divided into at least two subtypes (type IIa and type IIb). Type IIa LNs (LN IIa) have strong Ca^{2+} dependent active membrane properties and respond with odor specific complex patterns of excitation, sometimes including the generation of Ca^{2+} driven 'spikelets'. In contrast, type IIb LNs (LN IIb) respond mostly with sustained, relatively smooth depolarizations. Despite the fact that many potential transmitters and neuromodulatory substances have been detected in the AL, the morphologically and physiologically distinct LN subtypes remain to be unequivocally assigned to these biochemical profiles. Solving this challenge would allow a better understanding of the role of LNs in olfactory signal processing.

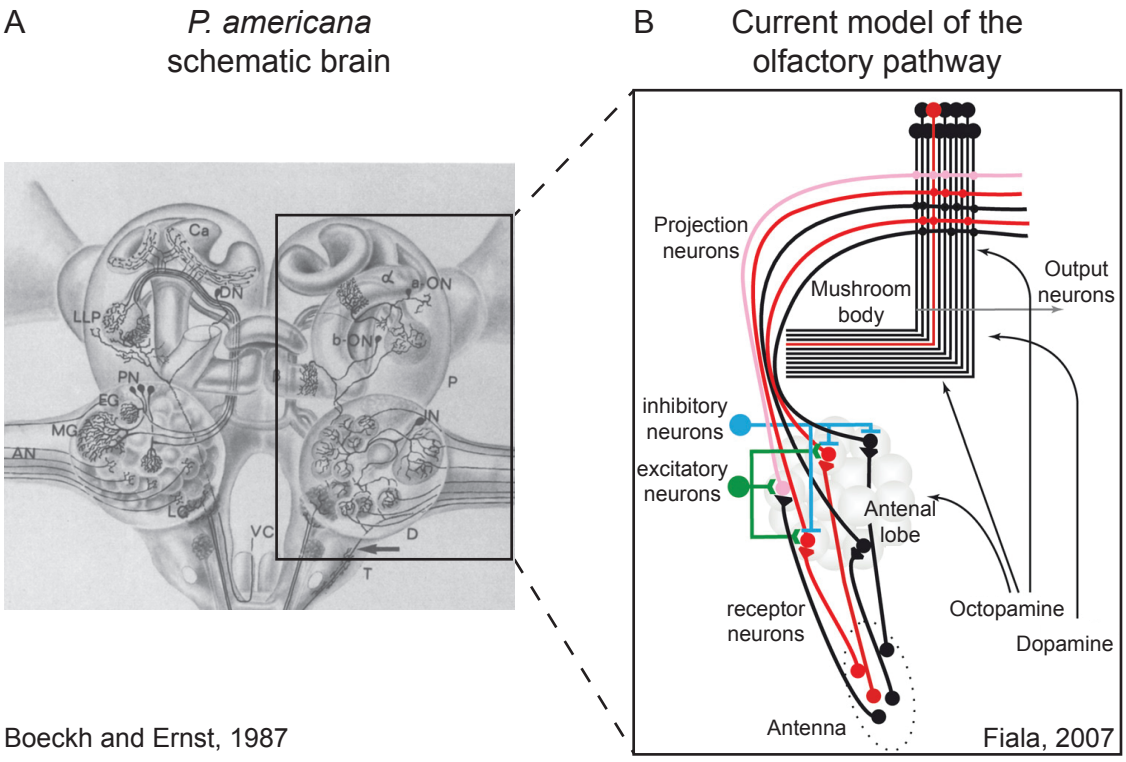

Figure 1.1. Current view on olfactory pathways in the insect brain. A, Chemosensory pathways in the brain of *P. americana*, taken from Boeckh & Ernst (1987). AN: antennal nerve, a(b)-ON: $\alpha(\beta)$-lobe output neuron, Ca: mushroom body calyx, D: deutocerebrum, DN: descending neuron, EG: glomerulus with cineole-sensitive projection neuron, IN: local interneuron, LG: lobus glorneratus, LLP: lateral lobe of the protocerebrum, MG: macroglomerulus, P: protocerebrum, PN: projection neuron, T: tritocerebrum, VC: ventral nerve cord, α: α-lobe of the mushroom body, β: β-lobe of the mushroom body. **B,** Exemplary wiring diagram of the olfactory pathway as proposed for *Drosophila* (taken from Fiala, 2007). Odors are perceived by olfactory receptor neurons located on the antenna which project to the antennal lobe (activated neurons are marked red). In the antennal lobe network, local inhibitory and excitatory neurons transform olfactory information so that projection neurons respond to a broader range of odorants compared to receptor neurons (illustrated by the pink PN, that is not activated by the respective receptor neuron, but by the excitatory LN). The transformed olfactory information is then relayed to mushroom body neurons by PNs.

1.3 Objectives of this thesis

The organization of potential neurotransmitters and -modulators of the antennal lobe has been studied in various species. In this thesis, for the first time, potentially neuroactive substances were unequivocally assigned to distinct, functionally different LN types. The specific objectives were:

1. To investigate the immunoreactivity for the biosynthetic enzyme choline acetyltransferase (ChAT), a marker for cholinergic neurons, in morphologically and electrophysiologically identified AL interneurons.

2. To analyze the cotransmitter- or modulator inventory of distinct LN types, concentrating on neuropeptides that were shown to be abundant in the AL through mass spectrometry.

3. To establish a method that allows Matrix-assisted laser desorption/ionization-time of flight mass spectrometry (MALDI-TOF MS) on single neurons to be performed subsequent to patch-clamp recording and single cell staining for unequivocal physiological and morphological identification. This will catalog the full range of potential neuroactive substances for individual neurons.

   This part was done in collaboration with Susanne Neupert and Axel Kersting of Reinhard Predel's group

2 Materials and Methods

Parts of this work were done in collaboration.
For peptide immunocytochemistry, animals were sent to Joachim Schachtners laboratory at the University of Marburg. Single labelings for peptides were made by Basil El Jundi and double labelings for GABA and AT as well as for GABA and TKRP by Martina Kern. Preparations were sent to me for data acquisition and analysis.
Gel electrophoresis and Western blotting were performed in collaboration with Arnd Baumann at the Research Center Jülich.

2.1 Animals

Adult cockroaches, *Periplaneta americana*, were obtained from a laboratory colony, kept under controlled conditions at 27°C with a photoperiod of 12 h light and 12 h dark. The animals were reared on an artificial diet of dried grass pellets for rodents, oat flakes and water.
All experiments were performed on adult males. Before dissection, the animals were anesthetized by CO_2 for $\sim$ 30 s and immobilized in a custom built preparation holder.

2.2 *In situ* preparation

The intact brain preparation was based on an approach described previously (Husch *et al.* , 2009a,b; Demmer & Kloppenburg, 2009), in which the entire olfactory system was left intact. The anesthetized animals were placed in a custom-

built holder and the head with antennae was immobilized with tape (Tesa Extrapower Gewebeband, Tesa, Hamburg, Germany). The head capsule was opened by cutting a window between the two compound eyes and the bases of the antennae. The brain with antennal nerves and antennae attached was dissected from the head capsule in 'normal saline' (see below) and pinned in a Sylgard-coated (Dow Corning Corp., Midland, Michigan, USA) recording chamber. To gain access to the recording site and facilitate the penetration of pharmacological agents into the tissue, the ALs were desheathed using fine forceps and bent dorsally, then the tissue was enzyme treated with papain (0.3 mg/ml; P4762, Sigma-Aldrich) and L-cysteine (1 mg/ml; 30090, Fluka) dissolved in normal saline [$\sim$ 3 min, room temperature (RT)]. For recordings, the somata of the AL neurons were visualized with a fixed-stage upright microscope (BX51WI, Olympus) using a 40x water-immersion objective [UMPLFL, 40, 0.8 numerical aperture (NA), 3.3 mm working distance, Olympus] and infrared- differential interference contrast optics. All chemicals, if not stated otherwise, were acquired from AppliChem (Darmstadt, Germany) in pro-analysae purity grade.

2.3 Electrophysiological recordings

2.3.1 Whole-cell patch-clamp recordings

Whole-cell voltage- and current-clamp recordings were performed at room temperature (22°C) closely following methods described by Hamill *et al.* (1981). Electrodes with a tip resistance of 2.5 - 3 MΩ were produced with a temperature controlled pipette puller (PIP5, HEKA, Lambrecht, Germany or PC-10, Narishige, Japan) from borosilicate glass capillary tubing (Science Products, GB150-8P, 0.86 x 1.5 x 80 mm). Whole-cell patch-clamp recordings were performed with an EPC9 or EPC10 patch-clamp amplifier (HEKA), controlled by the software Pulse v8x63 or Patchmaster v2x60 (HEKA) running on a personal computer under Microsoft Windows XP. The sample interval was 100 µs (10 kHz). The signal was filtered with a series combination of two low-pass Bessel filters with a cut-off frequency of

2.9 kHz and 10 kHz. In voltage-clamp, pipette and membrane capacitance were compensated using the automatic compensation circuit of the EPC9 or EPC10. To eliminate remaining linear leak and capacitative currents, a p/6 protocol (Armstrong & Bezanilla, 1974) was used.
For single cell staining the pipettes were filled with an internal solution containing [mM] 190 K-Aspartate, 10 NaCl, 1 $CaCl_2$, 2 $MgCl_2$, 10 HEPES, 10 EGTA, adjusted to pH 7.2 with KOH resulting in 415 mOsm and 1% biocytin. The liquid junction potential against the saline solution (Neher, 1992) was calculated with the Patcher's Power Tools plug-in for Igor Pro. The recorded data were analyzed using the software Pulse and Igor Pro v4.07.

2.3.2 Perforated patch-clamp recordings

Perforated patch-clamp experiments were performed using protocols modified from Akaike (1996); Könner *et al.* (2011). Electrodes with a tip resistance of 3.5 - 5 MΩ were used for recordings to quickly achieve a seal resistance of $\geq$1 GΩ. The patch pipette was tip filled with pure internal solution and back filled with biocytin and gramicidin containing internal solution to achieve perforated patch-clamp recordings. The ionophore gramicidin (G5002, Sigma) was dissolved in dimethyl sulfoxide (DMSO; D8418, Sigma) to a concentration of 10 µg/µl and added to the pipette solution resulting in a final concentration of 25 - 75 µg/ml. The used DMSO concentration (0.25 - 0.75%) had no obvious effect on the investigated cells. Recordings were performed with an EPC10 amplifier as described for whole-cell patch-clamp.

2.3.3 Odor stimulation

A continuous airflow system was used to deliver the odorants. Carbon-filtered, humidified air was guided across the antenna at a flow rate of 2 l/min ('main airstream') through a glass tube [10 mm inner diameter (ID)] that was placed perpendicular to and within 20-30 mm distance of the antennae. To apply odorants, 5 ml of odorant containing solutions [either pure or diluted in mineral oil

(M8410, Sigma)] were transferred into 100 ml glass vessels. Strips of filter paper in the odorant solution were used to facilitate evaporation. The concentration of each odorant in the mineral oil was adjusted to match the vapor pressure of the odorant with the lowest value (eugenol). Dilutions were as follows: α-ionone 72.2% (I12409, Aldrich), +/- citral 1.5% (C83007, Aldrich), citronellal 4.9% (W23071h, sigma), eugenol 100% (E51791, Aldrich), geraniol 78.2% (48799, Fluka), hexanol 1.1% (52830, Fluka). The headspace of pure mineral oil was used as a control stimulus (blank). During a 500 ms stimulus, 22.5 ml air of the main air stream was diverted through the odorant containing vessel by a solenoid valve system and reinjected into the airstream, ensuring a continuous airflow volume across the preparation. The solenoids were controlled by the D/A-interface of the EPC9 patch-clamp amplifier and the Pulse or Patchmaster software. Odorant-containing air was quickly removed from the experimental set-up with a vacuum funnel (3.5 cm ID) placed 5 cm behind the antennae. Consecutive odorant stimulations to the same preparation were performed with an interval of at least 60 s. Typically all six odorants were tested.

2.4 Single cell labeling and immunocytochemistry

2.4.1 Biocytin labeling

During recording in whole-cell configuration, the cell was loaded with 1% biocytin for $\sim$ 20 - 30 min by injecting a hyperpolarizing current of 0.2 - 0.6 nA.
In perforated patch configuration the investigated neurons were juxtasomal filled with biocytin by giving electroporating stimuli via the patch pipette. When a seal resistance of $\sim$1 GΩ was reached, a sequence of 5 - 10 500 ms trains of 1 ms square pulses with a frequency of 200 Hz and an amplitude of -1 V was given with an interstimulus interval of 5 s. Biocytin was then allowed to diffuse into the neurites for at least 20 min.
The brain was then fixed overnight at 4 °C in a commercially available fixative which consisted of 0.2 M phosphate buffered saline [(PBS), pH 7], containing 4%

formaldehyde (Roti-Histofix 4%, Roth, Karlsruhe, Germany). Subsequently, it was rinsed in PBS (3 x 20 min). To enhance the penetration of the biocytin binding streptavidin, the brain was enzyme-treated with 1 mg/ml collagenase-dispase (Roche Diagnostics GmbH, Mannheim, Germany) and 1 mg/ml hyaluronidase (Sigma-Aldrich), for 20 min at 37 °C . The treatment was terminated by rinsing the preparation in 4 °C PBS (3 x 10 min). To further enhance the streptavidin penetration, the brain was incubated for 45 - 60 min at RT in PBS containing 1% Triton X-100 (Serva, Heidelberg, Germany). The brain was then rinsed again in PBS (3 x 10 min) and incubated overnight at 4 °C in PBS containing Alexa Fluor 633 or DyLight 649 conjugated streptavidin (1:400, Molecular Probes, Eugene, OR) and 10% normal goat serum (Vector Labs, Burlingame, CA), to block unspecific streptavidin binding. Then, the brain was rinsed again in PBS and dehydrated in an ascending ethanol series (50, 70, 90, 2x 100%, 10 min each) before being cleared and mounted in methylsalicylate (Sigma-Aldrich).

Sectioning

After capturing fluorescence images of the whole-mount (see 2.4.3 Image Processing), the brain was rinsed for 10 min in 100% ethanol and then either stored in 70% ethanol until further processing or directly rehydrated in a descending ethanol series and embedded in agarose (4% in PBS, Serva, Heidelberg, Germany). Ventrodorsal sections (100 µm) were obtained with a vibratome microtome (HM-650 V, Thermo Scientific, Walldorf, German) in 4°C PBS. If the previous wholemount staining was weak, the slices were reincubated again overnight with streptavidin. After rinsing with PBS (3x 10 min), the slices were dried on 0.05% chrome-alum (Fluka) and 0.5% gelatin (Merck) coated slides, treated with xylene for 10 min to remove lipids and mounted in Permount (Fisher Scientific, Fair Lawn, NJ).
Slices where used to obtain high resolution detail images and could be stored.

Antigen	Antibody	Immunogen	Reference	Source
AST-A	[1]Dip-AST-7	APSGAQRLYGFGLa	Vitzthum *et al.* (1996)	H. Agricola (Jena, Germany)
AT	[2]Mas-AT-1	GFKNVEMMTARGFa	Veenstra & Hagedorn (1993)	J. Veenstra (Bordeaux, France)
ChAT	ChAT4B1	*Drosophila* ChAT fusion protein	Takagawa & Salvaterra (1996)	P.M. Salvaterra (Duarte (CA), USA)
GABA	anti-GABA	GABA-bovine serum albumin	Kolodziejczyk *et al.* (2008)	Sigma-Aldrich (Saint Louis (MO), USA)
MIP	[3]Pea-MIP-1	GWQDLQGGWa	Predel *et al.* (2001)	M. Eckert (Jena, Germany)
TKRP	[4]Lom-TK 2	APLSGFYGVR-NH2	Veenstra (1995)	J. Veenstra (Bordeaux, France)

Table 2.1. Primary antibodies used for immunocytochemistry.
[1] *Diploptera punktata*-AST-7
[2] *Manduca sexta*-AT-1
[3] *Periplaneta americana*-MIP-1
[4] *Locusta migratoria*-Tachykinin 2

2.4.2 ChAT-immunocytochemistry

Double labeling

To label individual cells, 1% biocytin was added to the pipette solution. After the electrophysiological recordings, the brains were fixed in Roti-Histofix for 2-3 h at room temperature. Subsequently the brains were rinsed in PBS (3 x 20 min and then for 12 h, RT). Most brains were processed as whole mount preparations. Selected brains were embedded in agarose (4%, Serva, Heidelberg, Germany) in PBS and 200 - 250 µm thick ventrodorsal sections were cut with a vibration microtome (HM-650 V, Thermo Scientific, Walldorf, Germany). To facilitate antibody and streptavidin penetration samples were treated with a commercially available collagenase/dispase mixture (1 mg/ml, 269638, Roche Diagnostics, Mannheim, Germany) and hyaluronidase (1 mg/ml, H3506, Sigma-Aldrich) in PBS (1 h, 37 °C), then rinsed in PBS (3 x 10 min, 4 °C) and then incubated in PBS containing 1% Triton X-100 (A1388, AppliChem) (PBS - 1%Tx) for 1 h at RT. Subsequently, the samples were incubated in PBS-based blocking solution containing 5% bovine serum albumin (BSA, A1391, AppliChem), 0.02 % sodium azide (S2002, Sigma-Aldrich), and 0.5 % Triton X-100 for 12 h at 4 °C. The brains were then incubated for one week (slices for 4 days) at 4°C with monoclonal mouse anti-Drosophila-

ChAT primary antibodies (ChAT4B1, dilution 1:50 in blocking solution). Non-bound primary antibodies were rinsed off in PBS - 1%Tx (20 min, RT) and PBS containing 0.5% Triton X-100 (PBS - 0.5%Tx, 2 x 2 h, RT). Detection of primary antibodies were performed with Cy 3- or DyLight 549-conjugated goat anti-mouse IgG (H+L) secondary antibodies (115-165-062; 115-505-146, Dianova, Hamburg, Germany). Secondary antibodies were diluted 1:200 in blocking solution supplemented with 5% normal goat serum (S-1000, Vector Labs, Burlingame, CA). Samples were incubated for 5 - 6 days (whole mount preparations) or 2 - 3 days (slices) at 4 °C. After rinsing in PBS-1%Tx (20 min, RT), PBS-0.5%Tx (2 x 2 h, RT) and PBS (3 x 10 min, RT), the brains were incubated with Alexa 633 conjugated streptavidin (1:400, S21375, Invitrogen, Eugene, OR) in PBS supplemented with 10 % normal goat serum for ∼12 h at 4 °C. Some preparations were counterstained with YO-PRO-1 (1:200 in streptavidin solution, Y3603, Invitrogen), rinsed in PBS (3 x 10 min, RT), dehydrated, cleared, and mounted in methylsalicylate.
For ChAT and GABA double-labeling, polyclonal rabbit anti-GABA primary antibodies (dilution 1:750, A2052, Sigma-Aldrich) were added to the ChAT4B1 antibody solution and incubated as indicated above. For anti-GABA antibody detection, Cy 2-conjugated goat anti-rabbit IgG (H+L) secondary antibodies (dilution 1:200, 111-225-003, Dianova) were added to the goat anti-mouse IgG (H+L) secondary antibodies used for ChAT4B1 detection.

2.4.3 Peptide immunocytochemistry

The general procedure followed the ChAT immunolabeling protocol (see chapter 2.4.2) with the following adjustments: The preparations were pre-incubated in blocking solution (∼3h, RT) containing 5% NGS, 0.02% and 0.5% Triton X-100 to block unspecific antibody bindings. Then the brains were incubated for one week (4°Cin rabbit anti-AT (*Manduca sexta*-AT, #. 13.3.91, 1:4000 in blocking solution) or rabbit anti-TKRP (*Locusta migratoria*-TKRP-2, ABD-045, Jena Bioscience, Jena, Germany), 1:40000 in blocking solution) (see table 1), and after rinsing, incubated in *DyLight*488 conjugated goat anti-rabbit IgG (H+L) secondary antibody (1:300,

5-6 days, 4°C, 111-485-045 Dianova, Hamburg, Germany) dissolved in blocking solution.

2.4.4 Antibody characterization

All antibodies, that were used in these studies are summarized in table 2.1. The expression of ChAT in cockroach neurons was examined with a monoclonal antibody (*ChAT4B1*) generated against a *Drosophila* ChAT fusion protein (Takagawa & Salvaterra, 1996). Characterization and specificity of the antibody has been examined by Takagawa & Salvaterra (1996) and Yasuyama *et al.* (1995). The versatility of this antibody to perform stainings in *P. americana* was examined by control experiments. On Western blots (see RESULTS) the antibody *ChAT4B1* recognized one band of $\sim$ 80 kDa in protein samples from Drosophila heads and a similar band in samples from *P. americana* brains. No staining was observed once the primary antibody was omitted.
A commercially available polyclonal antibody (A2052, Sigma) was applied that was raised against a GABA-BSA conjugate in rabbits to detect GABA in *P. americana* brain tissue. Control experiments were conducted to examine the staining specificity of the antibody: 1) Staining was abolished when the antibody was preincubated with 1 mM GABA (A2129, Sigma) and also 2) no staining of the samples was observed when the primary antibody was omitted.
Peptide-antisera, used here, were raised in rabbit against synthetic peptides (see Tab. 2.1 for respective immunogens). Specifities in *P. americana* brain tissue were confirmed by preabsorption of the antisera with the respective synthetic peptide (Predel *et al.* , 2001; Neupert *et al.* , 2012).

2.4.5 Image processing

Overview images of the whole-mount preparations were taken immediately after mounting in methylsalicylate with an LSM 510 Meta confocal laser scanning system (Carl Zeiss MicroImaging GmbH, Göttingen, Germany) mounted on a fixed stage inverse microscope (Zeiss Axiovert 100M equipped with 10x Plan-

Apochromat 0.45 NA, 20x Plan-Apochromat 0.75 NA, 40x oil-immersion Plan-Neofluar 1.30 NA, 63x oil-immersion DIC Plan-Apochromat 1.4 NA and 100x oil-immersion Plan-Neofluar 1.3 NA objectives).
Confocal images were captured using the multi track mode of the LSM 510 software. *DyLight 649/ Alexa 633*, *DyLight 549/Cy 3* and *DyLight 488/Cy 2* were imaged with 633 nm, 543 nm and 488 nm excitation, respectively. Emission of *DyLight 649/ Alexa 633*, *DyLight 549/Cy 3* and *DyLight 488/Cy 2* was collected through a 650 nm long pass, 560-613 nm band pass and 505-530 nm band pass filter respectively. Confocal images were adjusted for contrast and brightness and overlaid in ImageJ (version 1.42q). For overview pictures overlapping imaging stacks (10x) were merged in Photoshop CS5 (Adobe Systems Incorporated, San Jose, CA).

2.5 SDS-PAGE and western blotting

For gel electrophoresis and Western blotting, protein samples from the ALs of *P. americana*, an entire *P. americana* brain, *D. melanogaster* heads (positive control) and human embryonic kidney (HEK293) cells (negative control) were prepared. Brains of *P. americana* were dissected as described above. Flies were decapitated and the heads were used for protein preparation. About 10^7 HEK293 cells were used for protein preparation. The samples were homogenized in 50 µl lysis buffer containing (in mM): 10 NaCl, 25 HEPES, pH 7.5, 2 EDTA, protease inhibitor (1 mg/ml, Pefabloc (#76307), Sigma). Samples were centrifuged (18000 x g, 30 min, 4°C). The supernatants were collected and processed for gel electrophoresis according to Laemmli (1970). Proteins were separated on 10% SDS-polyacrylamide gels and transfered onto Immobilon-P PVDF membranes (Millipore, Schwalbach, Germany). Membranes were blocked in 5% non-fat dry milk in PBS buffer (PBS = 130 mM NaCl, 7 mM $Na_2HPO_4x2H_2O$, 3 mM $NaH_2PO_4xH_2O$) and then incubated with ChAT4B1 antibodies (dilution 1:500 in PBS containing 5% non-fat dry milk) for 12 h at 4 °C. The membrane was rinsed in PBS containing 0.02% Tween

20 (PBT, 4 x 15 min, RT) and then incubated with horse radish peroxidase (HRP)-conjugated goat-anti-mouse secondary antibodies (Sigma, Taufkirchen, Germany) at a dilution of 1:5000 in PBT for 1.5 h at RT. After several successive rinses with PBT and PBS, immunoreactive bands were detected with an ECL-Kit (GE Healthcare, Freiburg, Germany).

2.6 Tools for data analysis

The software Igor Pro 6.0.1 (Wavemetrics, including the Patcher's PowerTools plug-in) was used for analysis of electrophysiological data. Morphological data were analyzed using Amira 4.1.2 (Visage Imaging, Berlin) and the Skeleton Tree plug-in (Evers *et al.* , 2005). Colocalization analysis was performed in Volocity 5.2 (Perkin Elmer, Coventry; Barlow *et al.* 2010) by calculation of the product of the difference from the mean (PDM; equation 2.1) and Pearson's correlation coefficient (PCC, Manders *et al.* , 1993; Adler *et al.* , 2008; equation 2.2) for a pair of fluorescence images, where all pixels with the same image coordinates are paired.

$$PDM = (R_i - R_{av})(G_i - G_{av}) \tag{2.1}$$

$$PCC = \frac{\sum(R_i - R_{av})(G_i - G_{av})}{\sqrt{\sum(R_i - R_{av})^2 \sum(G_i - G_{av})^2}} \tag{2.2}$$

R_i is the intensity of one fluorophore in individual pixels and R_{av} the arithmetic mean of all the pixels, G_i and G_{av} are the corresponding values for the second fluorophore. PCC = 1 indicates a perfect correlation, -1 a perfect negative correlation and 0 no correlation. Values between -0.1 and 0.1 were considered 0. Two labeled structures were considered as co-localized at a PCC larger than 0.1. All calculated values are expressed as mean $\pm$ standard deviation (SD). For statistical analysis of data obtained for the different cell types, one-way ANOVA with Newman-Keuls post tests or unpaired t-tests were performed in Prism 5 (Graph-

Pad Software Inc., La Jolla, CA, USA). A significance level of 0.05 was accepted for all tests.

3 Results

The ALs are important synaptic relays for processing of olfactory information in the arthropod brain. Here, primary sensory input originating from odor detection by olfactory sensory neurons is processed. Excitatory and inhibitory local interneurons (LNs) are pivotal to mediate interactions between glomerular pathways, which shape the tuning profile of the uPNs. The uPNs then convey this processed information to higher brain centers. An important prerequisite for a detailed understanding of the functional role of olfactory LNs is to match the physiologically distinct LN subtypes with the variety of neurotransmitters and -modulators. Since the neurochemical identity of these LNs is not known in detail, yet, I combined patch clamp recordings and biocytin labeling of individual neurons with subsequent immunocytochemistry to explore the chemical profile of physiologically and morphologically identified LNs in the AL of *P. americana*.

3.1 Identification of antennal lobe neurons

Unequivocal identification of specific neuron types is a prerequisite to match neurochemical profiles with identified neurons. First, AL neurons were preidentified by the size and location of their somata within the VSG (Distler *et al.* , 1998), from which recordings were performed under visual control. The large majority of cell bodies in the ventral portion of the VSG belong to a homogeneous cluster of uniglomerular projection neurons (uPNs). Variously sized somata situated in the dorsal portion of the VSG belong mostly to LNs. Directly dorsal to the uPN somata is a relatively homogenous, densely packed soma group belonging to spiking type I LNs, whose neurites give rise to the Y-shaped tract and ex-

hibit GABA-like immunoreactivity (GABA-LIR) (Distler, 1989; Distler & Boeckh, 1997b; Husch *et al.* , 2009a). The somata located further dorsally belong mostly to a group of non-spiking LNs that are referred to as type IIa and type IIb LNs (Husch *et al.* , 2009a,b).

This pre-identification has proven to be effective for the major neuron types with a success rate of over 90%, and was verified in each case by the physiological and morphological characterization during and after the recording using the following criteria: The uPNs generate Na^+ driven action potentials upon stimulation with odors or depolarizing current injection and send their axons along the inner antenno-cerebral tract (iACT) to higher order brain structures (Malun *et al.* , 1993). Their morphology and response properties are well known in *P. americana* (Boeckh & Tolbert, 1993; Boeckh *et al.* , 1984; Distler *et al.* , 1998; Ernst & Boeckh, 1983; Ernst *et al.* , 1977; Lemon & Getz, 1998, 2000; Malun, 1991a,b). Among the LNs, two major types were identified by their distinctive physiological properties: 1) spiking type I LNs that generated Na^+ driven action potentials upon odor stimulation, and 2) nonspiking type II LNs, in which odor stimulation evoked depolarizations, but no Na^+ driven action potentials (Husch *et al.* , 2009a).

Type I LNs had arborizations in many, but not all glomeruli and the density of processes varied between glomeruli of a given type I LN. I showed that all LN I exhibited GABA-like immunoreactivity (GABS-LIR). Type II LNs apparently had processes in all glomeruli with density and distribution of arborizations that was similar in all glomeruli of a given type II LN, but varied between different type II LNs.

The nonspiking type II LNs can further be divided into two subtypes (type IIa and type IIb), which differed in the branch pattern within the glomeruli, the size and branch pattern of low order neurites, odor responses, active membrane properties, and the characteristics of voltage-activated calcium currents (Husch *et al.* , 2009b). Type IIa LNs had strong Ca^{2+} dependent active membrane properties and responded with odor specific elaborate patterns of excitation that could include Ca^{2+} driven 'spikelets' riding on the depolarization and periods of in-

hibition. In contrast, type IIb LNs responded mostly with sustained, relatively smooth depolarizations.

Both subtypes of LN II also had distinctive branch patterns and sizes of the primary and low order neurites (Fig. 3.1). For interglomerular communication within nonspiking local interneurons, which depend on passive electrotonic conductances of graded depolarizations, the neurite architecture connecting individual glomeruli might play an important role. Therefore, I analyzed the neurite organization for each LN II subtype by three dimensional reconstruction of the stained neurons in combination with a statistical analysis of the morphological data. I analyzed neurite length and diameter as well as the number of branchpoints between soma and individual glomeruli. Findings are summarized in a schematic representation of the neurite structure for both LN subtypes. In type IIa LNs, the neurites branched off the primary neurite in a regular, hierarchical pattern and the neurites eventually ended at the glomeruli (Fig. 3.1 A3). The branch pattern resulted in similar neuritic distances and a similar number of branch points between the glomeruli and the soma: for $\sim$ 95% of the glomeruli there were 3-6 branch points between the soma and a given glomerulus. Type IIb LNs had a branching pattern with multiple glomeruli being connected in a serial manner by thin neurites (Fig. 3.1 B3). The different branch pattern of type IIb LNs resulted in a more variable and potentially higher number of branch points between soma and glomeruli (Fig. 3.1 C). In general the lower order neurites were longer and thicker in type IIa as shown in figure 3.1 D. The 1st to 9th order neurites (except 3rd order) of type IIa LNs were significantly longer and thicker than in type IIb LNs ($p < 0.001$). This difference is particularly striking for the primary neurite (Fig. 3.1 A1, B1, D). Type IIa LNs always had a clearly defined primary neurite (length: 62.6 $\pm$ 20.2 µm; d = 7.4 $\pm$ 3.2 µm; n = 5; Fig. 3.1 A1,D), while the primary neurite was significantly shorter in type IIb LNs (length: 15.1 $\pm$ 6.8 µm; d = 3.4 $\pm$ 2.4 µm; n = 5; p = 0.001, Fig. 3.1 B1,D), where it was sometimes barely recognizable.

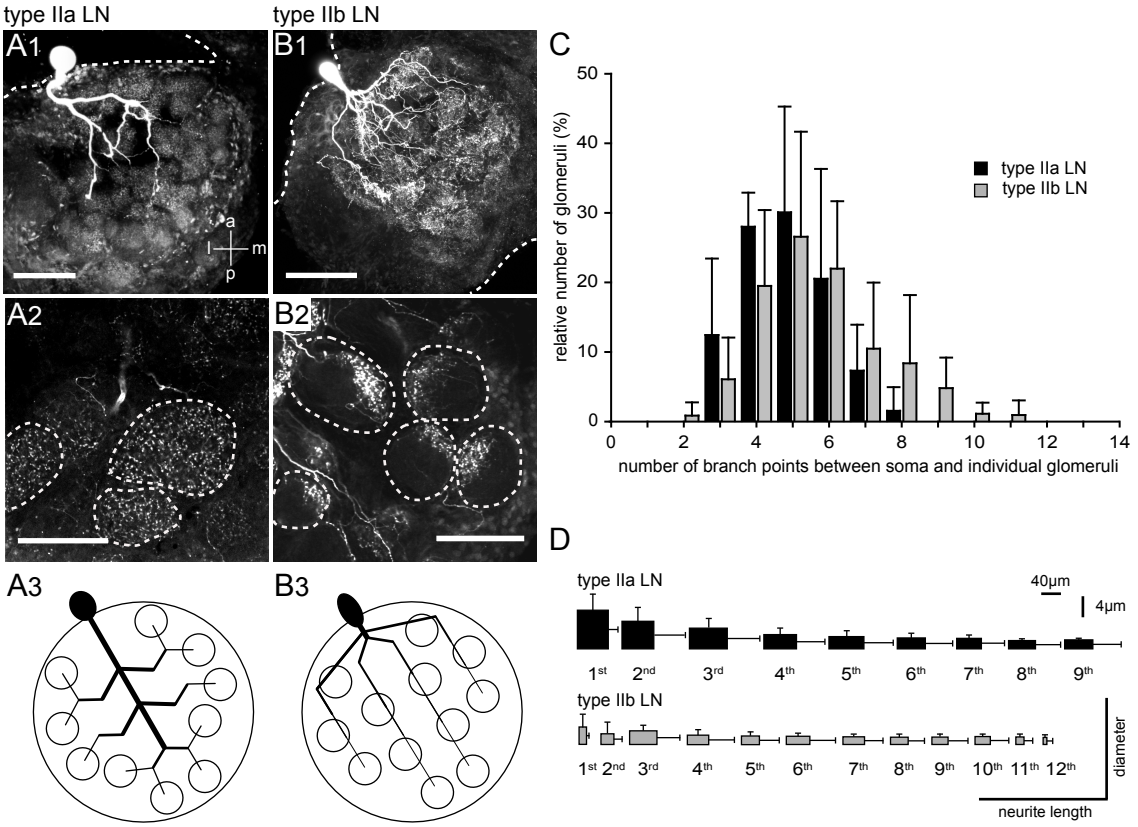

Figure 3.1. Morphological features of distinct LN II. The morphology of the recorded neurons was revealed by staining via the recording pipette. Type II neurons had arborizations apparently in all glomeruli, including the macroglomerulus. The density and distribution of processes were similar in all glomeruli of a given neuron, but varied within the glomeruli between neurons, as did the length and branching pattern of low order neurites. A1: type IIa LN (image stack, 145 µm). All glomeruli were homogeneously innervated, which is demonstrated in A2. B1: type IIb LN (image stack, 109 µm). All glomeruli were only partially innervated, which is demonstrated in B2. A3 and B3: Scheme of a type IIa and type IIb LN to demonstrate the different branching pattern. C: distribution of the number of branch points between the soma and randomly selected individual glomeruli from type IIa LNs (5 neurons; 117 glomeruli) and type IIb LNs (5 neurons; 166 glomeruli). D: length and diameter of the primary and the consecutive higher order neurites (numbers indicate the order) of type IIa and type IIb LNs. 1st to 9th order neurites (except 3rd order) were significantly longer and thicker in type IIa LNs ($p < 0.05$ for each order). Scalebars: A1, B1, 100 µm; A2, B2, 50 µm.
(taken from Husch *et al.* , 2009b, data in A and B by Moritz Paehler and Andreas Husch)

3.2 ChAT-like immunoreactivity in identified local interneurons

Physiological studies in *Drosophila melanogaster* suggest that important excitatory interactions between glomerular pathways are mediated by cholinergic LNs (Olsen *et al.* , 2007; Root *et al.* , 2007; Shang *et al.* , 2007; Chou *et al.* , 2010; Das *et al.* , 2008; Huang *et al.* , 2010; Seki *et al.* , 2010; Silbering & Galizia, 2007). Given the functional relevance of this excitatory interaction, it seems likely that such connections may also exist in other species. Currently it is not known which if any, functional subtype of LNs in *P. americana* may contain and release acetylcholine. By using an antibody against the biosynthetic enzyme choline acetyltransferase (ChAT) as a marker for cholinergic neurons I identified a subset of the nonspiking type IIa LNs with distinct physiological and morphological properties as cholinergic.

3.2.1 Antibody specificity

An antibody raised against the *Drosophila* choline acetyltransferse (*ChAT4B1*) was used to identify cholinergic neurons. Although the specificity of this antibody has been demonstrated for the fruit fly (Takagawa & Salvaterra, 1996), I first tested whether the antibody recognized an orthologous protein from *P. americana*. Western blots containing protein homogenates from *P. americana* ALs, *D. melanogaster* heads, and HEK293 cells was tested with *ChAT4B1* antibodies (Fig. 3.2). In the *D. melanogaster* sample (Fig. 3.2, lane 1), the antibody labeled a band of the expected size ($\sim$ 80 kDa; Slemmon *et al.* 1991). In the *P. americana* sample (Fig. 3.2, lane 2) a band of a similar molecular weight was observed, suggesting that an orthologous enzyme is expressed in the *P. americana* brain. No signal was observed in the HEK293 cell sample serving as a negative control in this experiment (Fig. 3.2, lane 3).

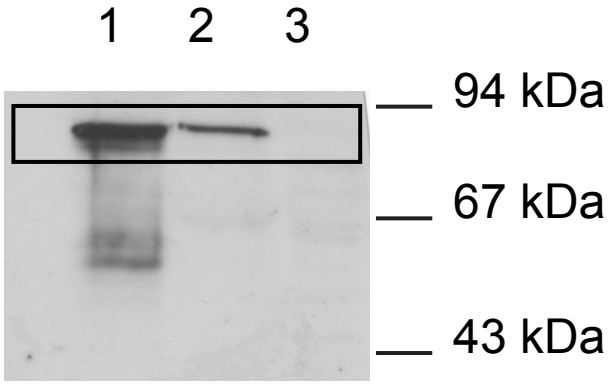

Figure 3.2. Western blot analysis of choline acetyltransferase expression. Protein samples of *D.melanogaster* heads (lane 1; positive control), *P. americana* antennal lobes (lane 2), and HEK293 cells (lane 3; negative control) were incubated with the monoclonal antibody *ChAT4B1*. The molecular weight is indicated on the far right. In the samples of *D. melanogaster* and *P. americana* a protein of $\sim$ 80 kDa was specifically labeled (black frame).

3.2.2 Immunocytochemical staining of wholemount preparations

In the first set of experiments, wholemounts were incubated with different combinations of antisera against ChAT and GABA, and the DNA stain *YO-PRO-1* to provide an overview of the distribution of ChAT-like immunoreactivity (ChAT-LIR) in the deutocerebrum (Fig. 3.3).

ChAT-LIR was observed exclusively in a small population of somata (Fig. 3.3A). While the neuropile was not labeled, I found ChAT-LIR in the ventral region of the VSG, a region where uPN somata are located (Fig. 3.3 A, B_A). In the dorsal region of the VSG, where mostly somata of type II LNs are located, ChAT-LIR was more scattered (Fig. 3.3 B_B, B_C).

The type I LN soma group directly dorsal of the uPN somata showed GABA-LIR, but not ChAT-LIR (Fig. 3.3 B_B).

Notably, there was no colocalization of the *YO-PRO-1* label and ChAT-LIR. This is due to fact that the labeled molecules (DNA and ChAT) are located in different cellular compartments. While ChAT is synthesized and eventually processed in the cytosol, the DNA is enclosed by the nuclear envelop. In figure 3.3 A ChAT-

LIR is labeled in red and the DNA stain *YO-PRO-1* is depicted in green. Yellow regions in Figure 3.3 A, originating from overlapping red and green staining, however, are caused by the projection of image stacks with red (ChAT) and green (DNA) labels into one two-dimensional plane and thus are not caused by a physical colocalization of DNA and ChAT.

Based on these staining patterns I hypothesized that, besides in the uPNs, ChAT-LIR is located in a subpopulation of type II LN somata. This was verified by studying identified AL neuron types by whole cell patch clamp recordings combined with single cell labeling and immunocytochemistry.

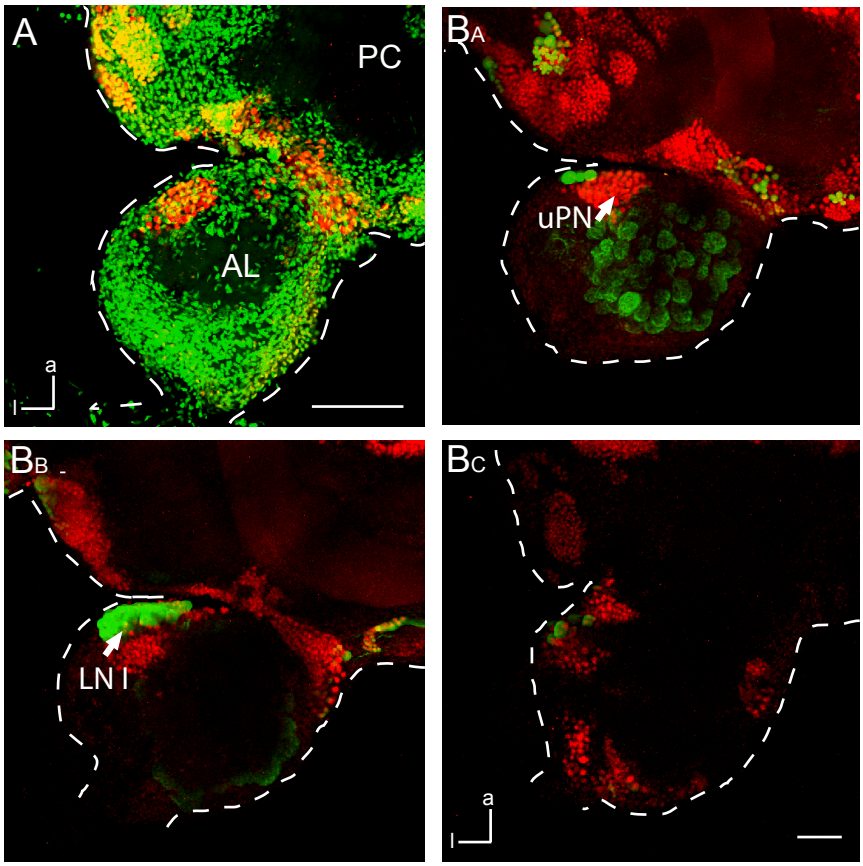

Figure 3.3. ChAT- and GABA-like immunoreactivity in the antennal lobe. A, Overview. Chat-LIR (red) labeled defined populations of neuronal somata in the AL. To aid orientation the DNA-specific label YO-PRO-1 (green) marked the nuclei of neurons and glia cells in the AL (95 µm image stack). **B_A-B_C**, ChAT-LIR (red) and GABA-LIR (green) in the ventral (B_A, 190 µm image stack), the medial (B_B, 130 µm image stack) and the dorsal region (B_C, 150 µm image stack) of the AL. Both labels did not colocalize. ChAT-LIR was located in the region of the uPN somata and GABA-LIR in the region of the type I LN somata. Scalebars: A, 100 µm; B_A-B_C, 50 µm.

3.2.3 ChAT-like immunoreactivity in nonspiking LN II

Nonspiking type II LNs exist in two subtypes. Type IIa LNs innervated all glomeruli homogeneously and had strong Ca^{2+} dependent active membrane properties and responded with odor specific elaborate patterns of excitation that could include Ca^{2+} driven 'spikelets' riding on the depolarization and periods of inhibition. Type IIb LNs innervated all glomeruli only in parts and responded mostly with sustained, relatively smooth depolarizations.
A total of 20 type IIa (Fig. 3.4 A, B) and 5 type IIb LNs (Fig. 3.4 C) were identified by their morphological and intrinsic electrophysiological properties and tested for ChAT-LIR. Whereas none of the type IIb LNs displayed ChAT-LIR (Fig. 3.4 C_D, 3.5), I found ChAT-LIR in 40% (8 out of 20) of type IIa LN somata, where it was restricted to regions of the soma. A co-localization analysis for the ChAT-LIR and the single cell label confirmed that ChAT-LIR was indeed located inside the somata (Fig. 3.4 A_{D1}, 3.5 A). Interestingly, type II LNs, which exhibited ChAT-LIR, also generated Ca^{2+} driven spikelets upon odor stimulation (Fig. 3.4 A_E). In contrast, type II LNs that were not stained by the ChAT4B1 antibody did not give rise to Ca^{2+} spikelets upon current injection or odor stimulation (Fig. 3.4 B_E, C_E).

In prior studies it was assumed that type IIa LNs have a similar gross morphology (see Husch *et al.* 2009b), yet a detailed inspection of ChAT-stained and ChAT non-stained type II LNs revealed clear differences in both, the soma size and the diameter of low order neurites. The whole-cell membrane capacitance (CM), which (mostly) reflects the soma size, was significantly smaller in ChAT-stained type IIa LNs (CM=83.0 $\pm$ 21.04 pF, n = 7) than in non-ChAT-stained type IIa LNs (CM=123.1 $\pm$ 36.5 pF, n = 9, P = 0.0218). Furthermore, the diameter of the first to third order neurites were significantly larger in type IIa LNs expressing ChAT-LIR (Fig. 3.6). In summary, two subclasses of nonspiking type IIa LNs could be distinguished.

1. Type IIa1 LNs exhibit ChAT-LIR, generate Ca^{2+} spikelets upon depolariza-

tion, possess (relative) small somata (CM ∼80 pF) and large diameter low order neurites.

2. Type IIa2 LNs do not exhibit ChAT-LIR, do not generate Ca^{2+} spikelets upon depolarization, possess larger somata (CM ∼125 pF) and small diameter low order neurites.

Figure 3.4 ***(following page).*** **ChAT-like immunoreactivity in a subpopulation of nonspiking LN II. A-C** show different subtypes of nonspiking type II LNs that exhibited or did not exhibit ChAT-LIR. The neurons were electrophysiologically characterized, labeled with biocytin/sreptavidin *Alexa 633* (red) and tested for ChAT-LIR (green) $\mathbf{X_A}$ Image of the entire neuron. $\mathbf{X_{B\text{-}D}}$ Soma of the neuron from X_A (frame) showing the biocytin/streptavidin (red) in X_B, the ChAT-LIR (green) in X_C and both labels overlaid (yellow) in X_D If colocalisation of both labels is indicated, the product of the differences from the mean (PDM) for each voxel of the two channels is shown in X_{D1}. $\mathbf{X_{E\text{-}F}}$ show current clamp (X_E and voltage clamp (X_F recordings to demonstrate the neuron specific intrinsic electrophysiological properties. The oscillations at the beginning of the voltage steps are generated by an interplay of outward K^+ currents and inward Ca^{2+} currents in regions of the neurons without perfect voltage control (Husch *et al.* , 2009a).
A, Type IIa1 LNs exhibited ChAT-LIR in the soma. Odor stimulation evoked a depolarization that gave rise to Ca^{2+} driven spikelets, but not to Na^+ driven action potentials. Depolarizing voltage steps evoked Ca^{2+} inward and K^+ outward currents, but no transient Na^+ inward currents ($A_{E\text{-}F}$, data provided by Andreas Husch). **B, C** Type IIa2 (B) and type IIb LNs (C) did not exhibit ChAT-LIR. Both neuron types generated depolarizations, but no Ca^{2+} driven spikelets or Na^+ driven action potentials during stimulation with odors. Depolarizing voltage steps did not evoke a transient Na^+ inward current. Scalebars: X_A, 100 µm; $X_{B\text{-}D}$, 50 µm

type IIa1

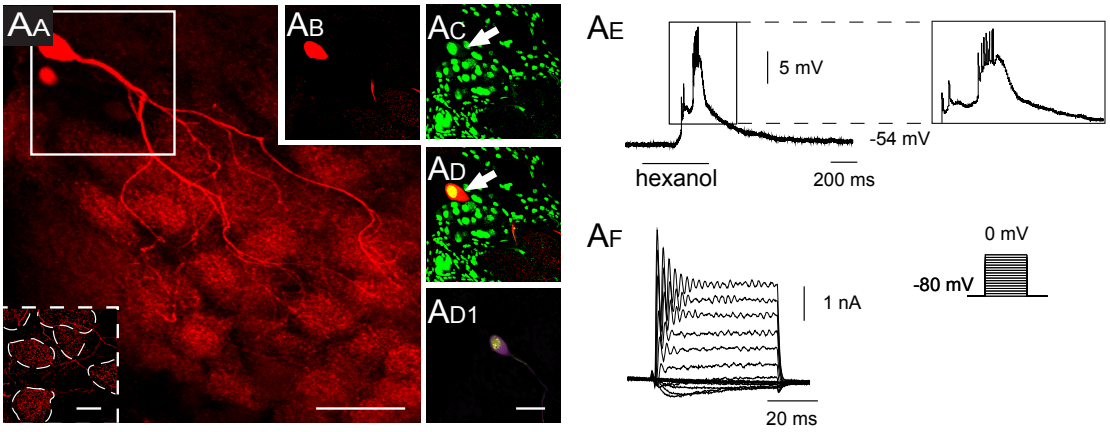

type IIa2

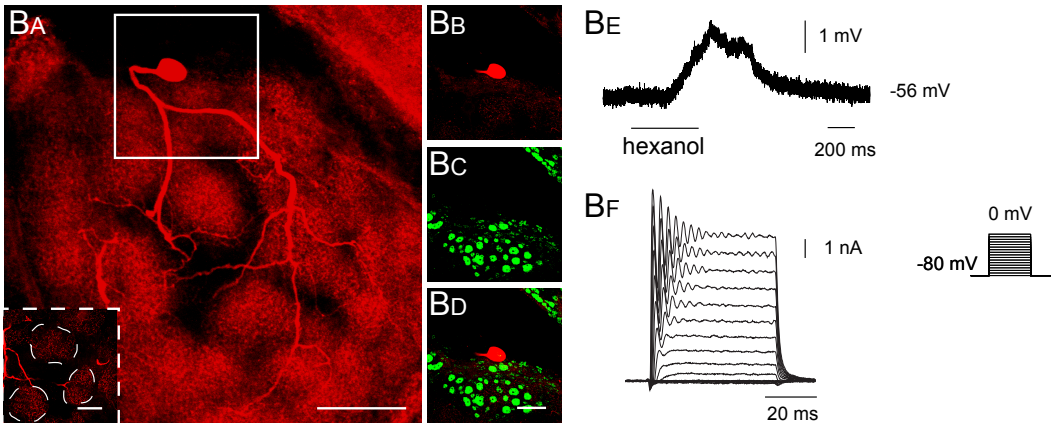

type IIb

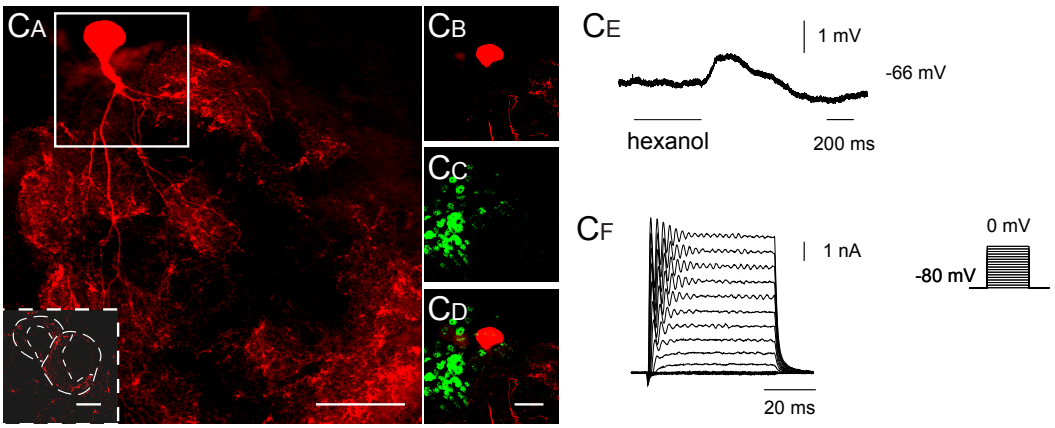

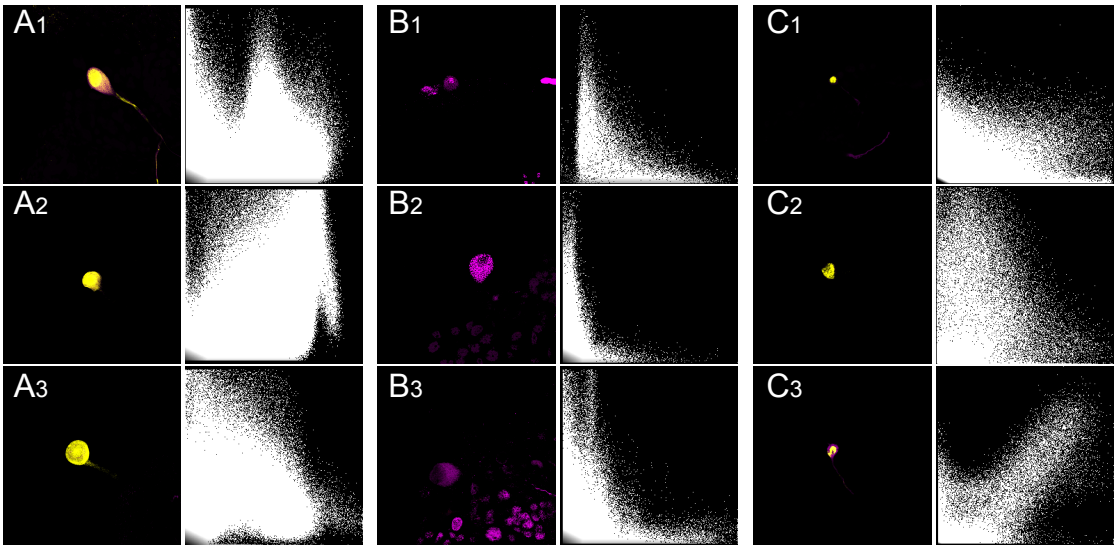

	LN IIa1	LN IIa2	LN IIb	LN I	uPN
LN IIa1		**	*	*	ns
LN IIa2	**		ns	ns	*
LN IIb	*	ns		ns	*
LN I	*	ns	ns		*
uPN	ns	*	*	*	

Figure 3.5. Colocalization analysis. A-C, PDM values (left) and scatter plots (right, x = intensity of ChAT-LIR, y = intensity of the biocytin/streptavidin label) of three exemplary confocal laser scans of single biocytin/streptavidin stained LN IIa1 (A_1-A_3), LN IIa2 (B_1-B_3) and uPN somata (C_1-C_3) showing ChAT-LIR. LN IIa1 somata and uPN somata show positive PDM values (indicated in yellow). Biocytin thus is colocalized with ChAT. LN IIa2 somata show negative PDM values (indicated in purple). Biocytin thus is not colocalized with ChAT. **D** Box plot of PCCs of each interneuron type (D_1) and summary of significances (D_2; $* = p \leq 0.05$, $** = p \leq 0.01$) .

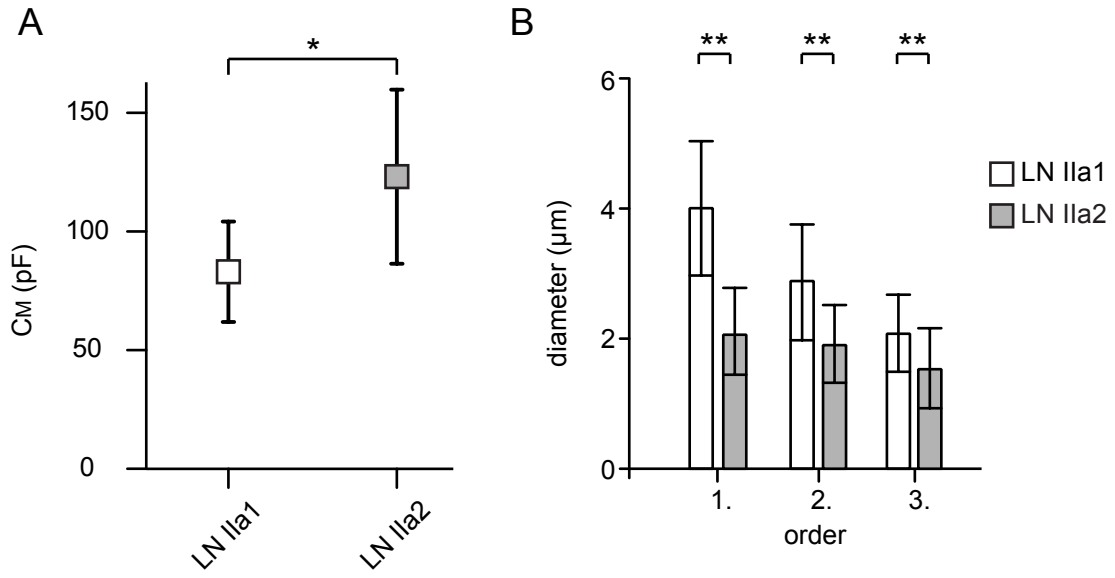

Figure 3.6. Morphological properties of type IIa LNs. A, The somata of type IIa1 LNs are significantly smaller than type IIa2 LN somata. This is demonstrated by the difference in whole cell capacitance (CM). **B**, The first to third order neurites are thicker in type IIa1 LNs compared to type IIa2 LNs

3.2.4 ChAT-like immunoreactivity in spiking LN I and uPNs

Immunocytochemical studies for ChAT, protein conjugated choline and choline transporter as well as acetylcholine esterase histochemistry in several insect species including *D. melanogaster, M. sexta, A. melifera* and *S. gregaria* suggest that uPNs are cholinergic (Buchner *et al.* , 1986; Kitamoto *et al.* , 1992; Homberg, 1994; Bicker, 1999; Homberg, 2002), while type I LNs selectively express GABA-LIR (Distler, 1989; Husch *et al.* , 2009a) and thus are most likely not cholinergic. To confirm this hypothesis, I tested the presumably cholinergic uPNs with axons in the iACT as well as the GABA-lir spiking LN I for ChAT-LIR, using whole cell patch clamp recording and single cell labeling with subsequent ChAT antibody staining.

Analysis of type I local interneurons

The clear separation of ChAT-LIR and GABA-LIR in the VSG (Fig. 3.3 B) suggested that the GABA-lir spiking type I LNs do not express ChAT-LIR. This result was further supported by the single cell analysis of type I LNs (n=7), which were identified by their morphological and intrinsic electrophysiological properties, and did not exhibit ChAT-LIR (Fig. 3.7, 3.5 D). These findings strongly support the notion that spiking type I LNs are not cholinergic.

Analysis of uniglomerular projection neurons

I found strong ChAT-LIR in the ventral somata of the VSG. Previous work in *P. americana* has shown that these cell bodies belong to a homogenous population of uPNs that send their axons via the iACT into the protocerebrum (Husch *et al.* , 2009a; Malun *et al.* , 1993). This is consistent with my analysis of ChAT-LIR in individual neurons whose somata are located in the ventral region of the VSG. All of these neurons were identified as uPNs which sent their axons into the iACT and expressed ChAT-LIR in their somata (n=4) (Fig. 3.8).

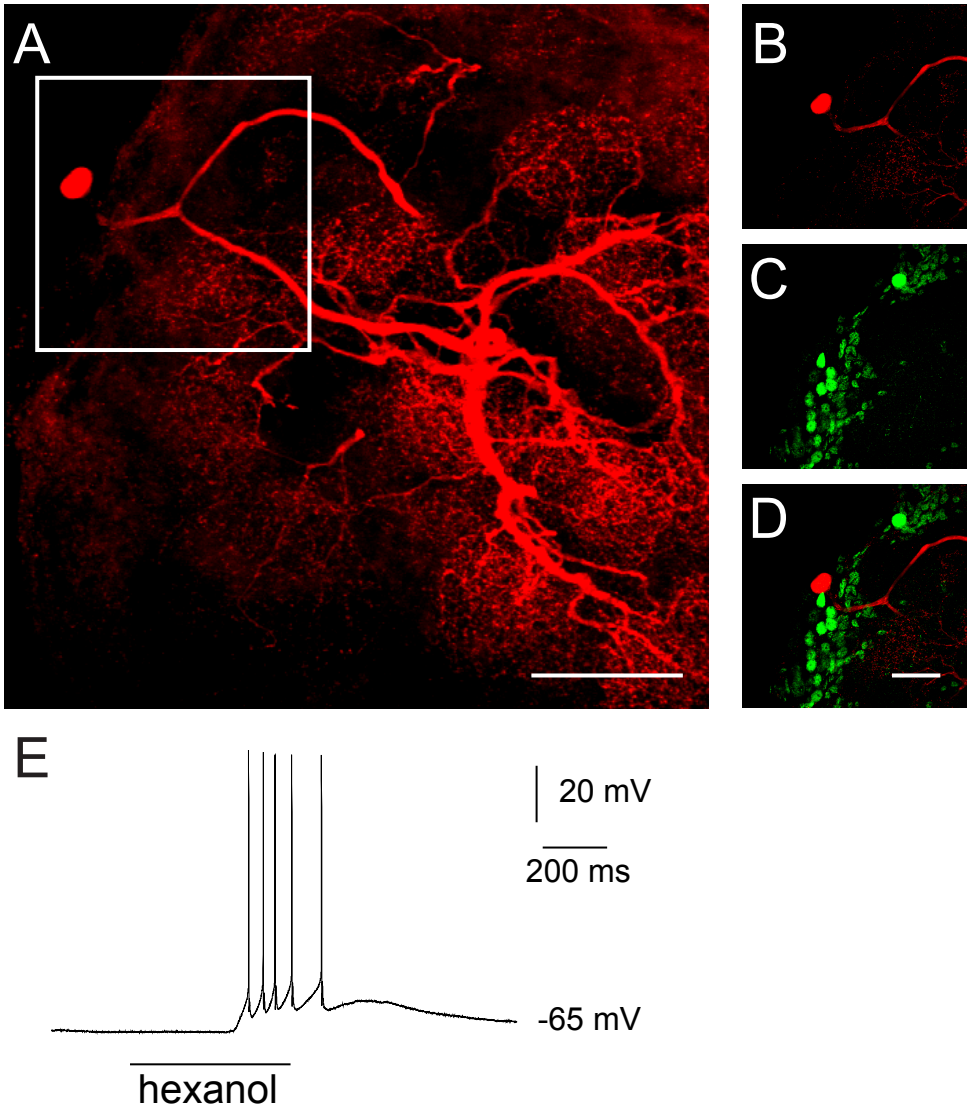

Figure 3.7. Spiking type I local interneurons do not express ChAT-LIR. A type I LN was labeled with biocytin/streptavidin (**A,B**, red) and tested for ChAT-LIR (**C**, green). No double labeling (**D**) was detected thus the neuron did not exhibit ChAT-LIR. **E**, Odor stimulation evoked Na^+ driven action potentials. Scalebars: A, 100 µm; B-D, 50 µm

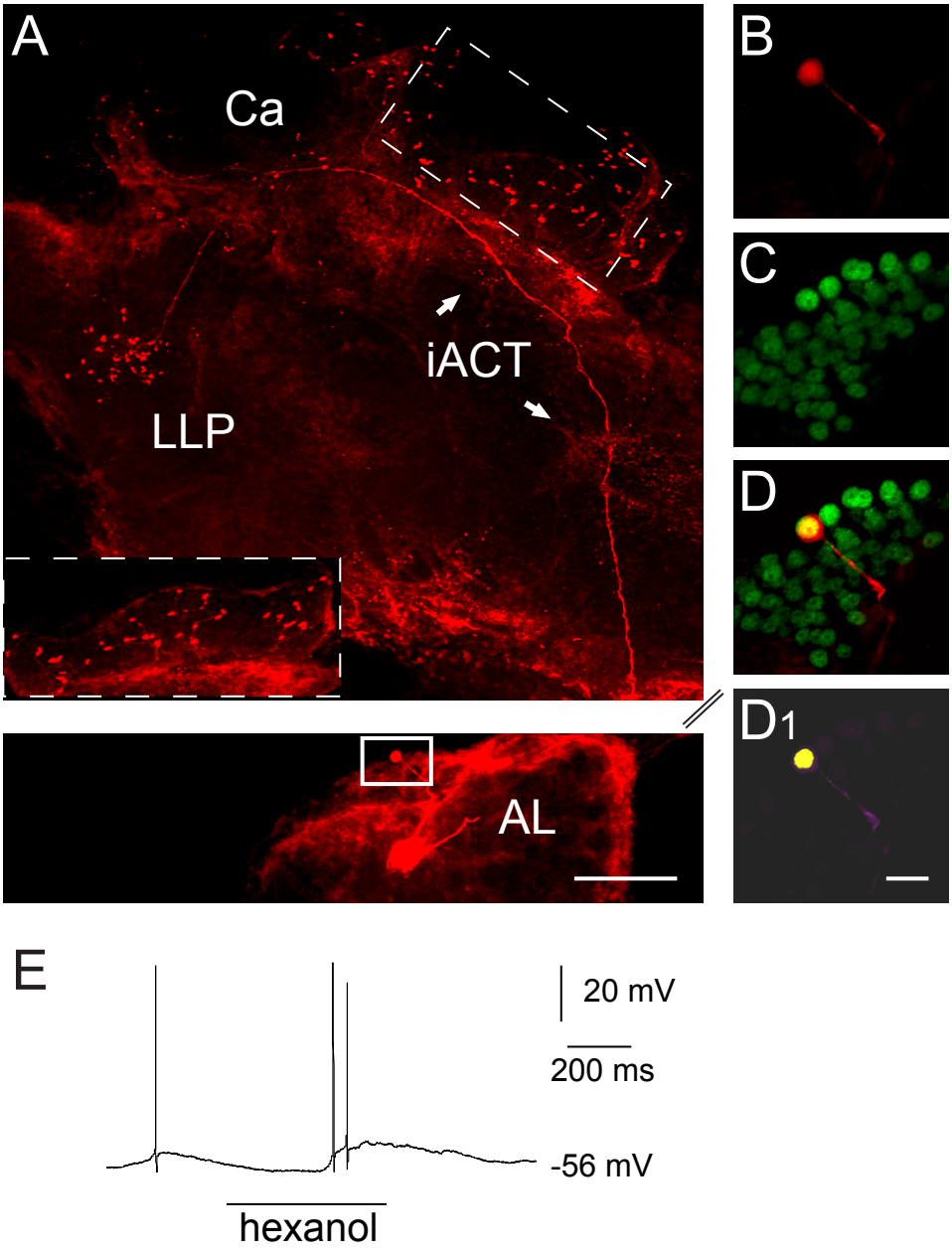

Figure 3.8. Uniglomerular projection neurons express ChAT-LIR. A uPN (**A**) was labeled with biocytin/streptavidin (**B**, red) and tested for ChAT-LIR (**C**, green. ChAT-LIR was detected in the soma as indicated by double labeling (**D**, yellow) and PDM values for each voxel of the two channels ($\mathbf{D_1}$). **E**, odor stimulation evoked Na^+ driven action potentials. Scalebars: A, 100 µm; B-D, 20 µm

3.3 Neuropeptide expression in local interneurons

Historically, based on immunocyto- and histochemical studies, LNs have been regarded as mostly GABAergic and inhibitory. However, by using several approaches, including immunocytochemical, mass spectrometrical and physiological studies, it became increasingly clear that the AL might contain a much larger variety of putative neuroactive substances. A major family of putative neurotransmitters and -modulators is that of the neuropeptides.(reviewed in Homberg, 1999a; Nassel & Homberg, 2006; Utz *et al.* , 2007; Nässel & Winther, 2010). While various neuropeptides have been detected in the AL of different insects, the exact expression pattern in functionally different LN types has still to be revealed.

Comparing the antibody stainings with the known location of the different neuron types is a good indicator of which interneuron type might match the immunoreactivity. Yet to unequivocally determine which interneuron type contains a certain neuropeptide, candidate neurons need to be identified physiologically and morphologically prior to immunocytochemical stainings. This kind of experiments, however, requires a clustered distribution of immunoreactive somata, to get a sufficient success rate. Hence, I first studied the distribution pattern of peptid immunoreactivity and then focused immunocytochemical experiments in identified interneurons on two neuropeptide families, which were most abundant in the VSG.
By using various combinations of antibodies against GABA, ChAT and diverse peptides, I showed allatotropin (AT) to be coexpressed with GABA in a subpopulation of LN I and tachykinin-related peptides (TKRPs) to be coexpressed with GABA in a subpopulation of LN I as well as with ACh in a subpopulation of LN IIa1.

3.3.1 Analysis of immunocytochemically stained whole-mount preparations

Mass spectrometric analysis of the ALs of *P. americana* provided a list of numerous peptides from 8 neuropeptide gene families that are present in the AL: allatostatins (AST-A), myoinhibitory peptide (MIP/AST-B), allatostatin (AT), FMRFamide-related peptides (FaRP; myosuppressin [LMS], short neuropeptides F [sNPF], extended FMRFamides [eFMRFa]), crustacean cardioactive peptide (CCAP) and tachykinin-related peptides (TKRP) (Neupert *et al.* , 2012). To get an initial overview of the gross distribution of the different neuropeptides in the AL, I prepared confocal fluorescent image stacks of the AL from wholemount preparations, that were incubated in antisera against AT, TKRP, AST-A and MIP/AST-B. Immunoreactivity of peptides that were of low abundance in the AL (LSM, eFMRFa, CCAP) was not tested. The description will be focused on the VSG somata.

Allatotropin

While the ventral portion of the VSG, where uPN somata are located remained unstained (Fig. 3.9 A_1), AT-lir somata formed a cluster apparently identical to that of the GABAergic LN I. Additionally, AT-LIR was detected in the y-shaped tract that is formed by LN I (Fig.3.9 A_2, B). Besides the somata in the presumed LN I cluster, in all preparations a single large diameter soma (35 - 40 µm) was prominent in the dorsal portion of the VSG (Fig. 3.9 A_3). The location of the soma, its diameter and the organization of the low order neurites suggest that this particular neuron belonged to the type IIb LNs (see Fig. 3.1 B). All glomeruli were invaded by varicose AT-lir fibers.

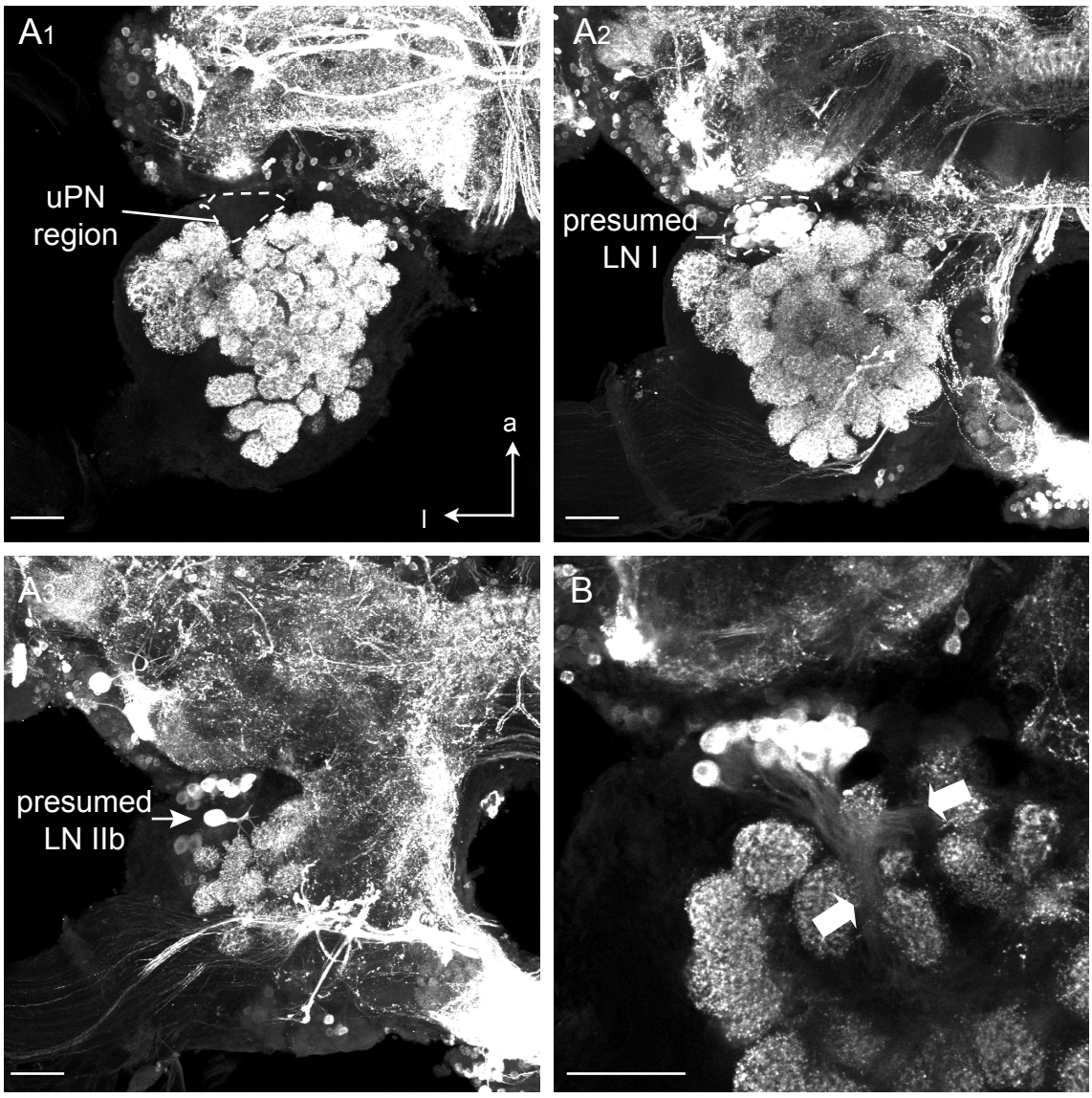

Figure 3.9. Distribution of AT-LIR in the antennal lobe. A, Overview of AT-LIR in the ventral (A_1), medial (A_2) and dorsal (A_3) region of the AL. A_1, No staining was observed in the uPN soma group. AT-LIR was expressed in a cluster in the region of LN I somata (A_2) and in a soma of a putative type IIb LN (A_3). **B**, Detailed view of the soma region in A_2 showing the for LN I typical y-shaped tract (arrows). Scale bars: 100 µm

Tachikinin-related peptides

At first glance the overall staining pattern of the anti-TKRP antibody preparations was similar to that of the anti-AT preparations. No immunoreactivity was detected in the uPN soma cluster (Fig. 3.10 A_1). A cluster of TKRP-ir somata was found in the region of the type I LN soma cluster (Fig. 3.10 A_2). Additionally, 6 - 12 immunoreactive somata were located dorsally to the presumed LN I cluster, in a region where LN II somata are located (Fig. 3.10 A_3). All glomeruli were invaded by varicose TKRP-lir fibers.

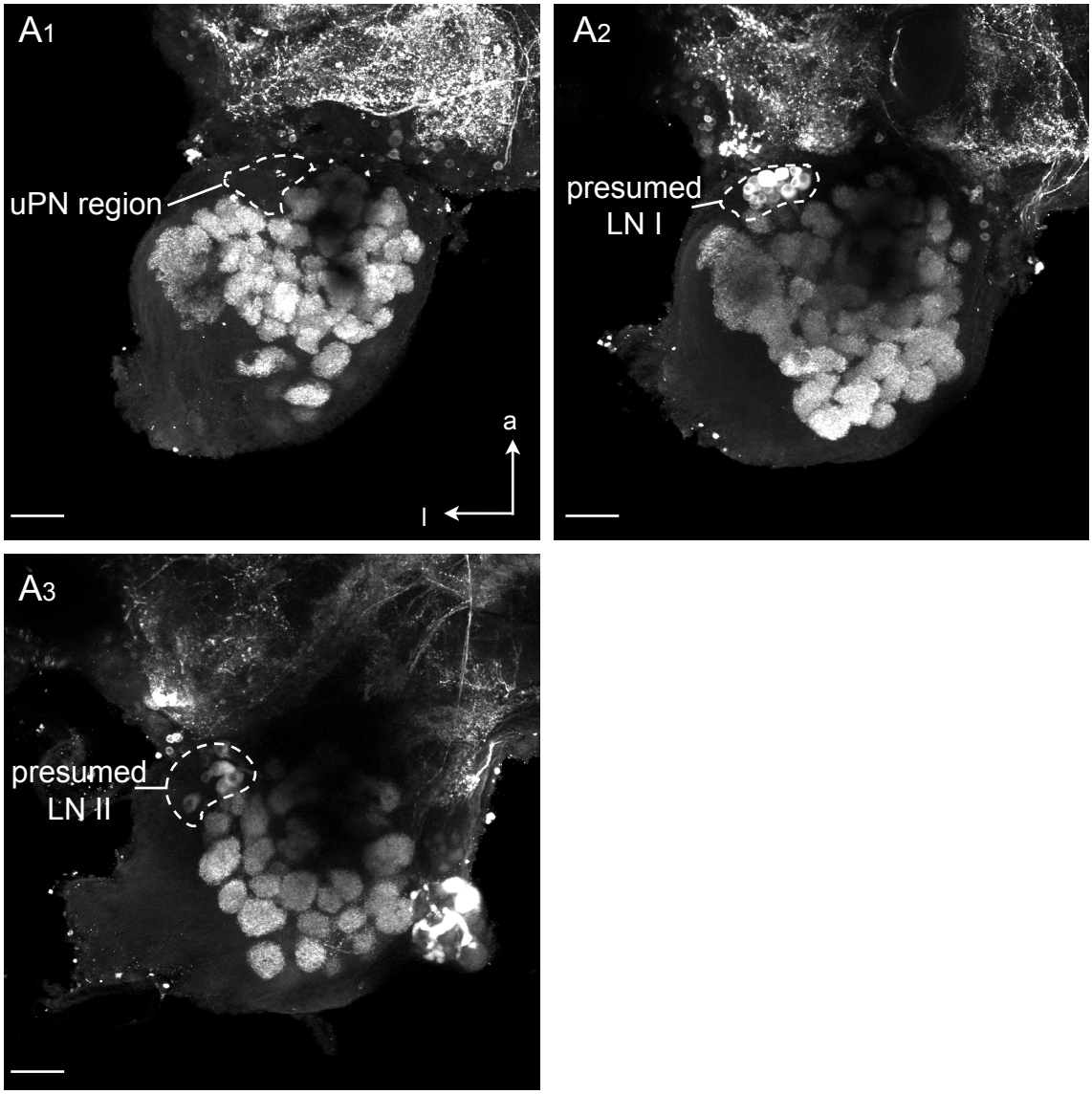

Figure 3.10. Distribution of TKRP-LIR in the AL. A, Overview of TK-LIR in the ventral (A_1), medial (A_2) and dorsal (A_3) region of the AL. A_1, No TKRP-LIR was observed in the uPN soma group. TKRP-LIR wass expressed in the region of LN I somata (A_2) as well as LN II somata (A_3). Scalebars: 100 µm

Allatostatin A

AST-A-LIR was scattered throughout the VSG and the somata were weakly stained for the most part, making it difficult to assign the somata to a particular cluster. 5 - 7 weakly stained somata were found in the region of the soma cluster were uPNs with projections in the iACT are located (Fig. 3.11 A_1), and about 15 AST-A-lir somata of various sizes and intensities of immunoreactivity were located in the dorsal portion of the VSG (Fig. 3.11 $A_{2,3}$). In the protocerebrum AST-A-lir fibers were detected in the iACT (Fig. 3.11 B_1) and ACT IV (B_2), suggesting PNs with projections in these tracts to express AST-A. The ACT IV comprises projections of multiglomerular projection neurons (mPNs) with somata located directly anterior to the entrance of the antennal nerve (AN) (Malun *et al.* , 1993). Size and location of these mPN somata match the strongly AST-lir somata that were found in the dorsal portion of the VSG, directly anterior to the AN (Fig. 3.11 A_3). Additional immunoreactivity was detected in axons of the antennal nerve (AN) that run into the antennal and dorsal lobe. Innervation of the glomeruli was restricted to the periphery of each glomerulus.

Aside from the VSG, a distinct cluster at the posterodorsal rim of the deutocerebrum was marked by the AST-A antiserum, that harbored $\sim$20 small diameter somata (Fig. 3.11 B). Processes of these hitherto unknown neurons could be traced to the AL through a prominent T-shaped tract that was first described in Neupert *et al.* (2012, Appendix Fig. 5.1).

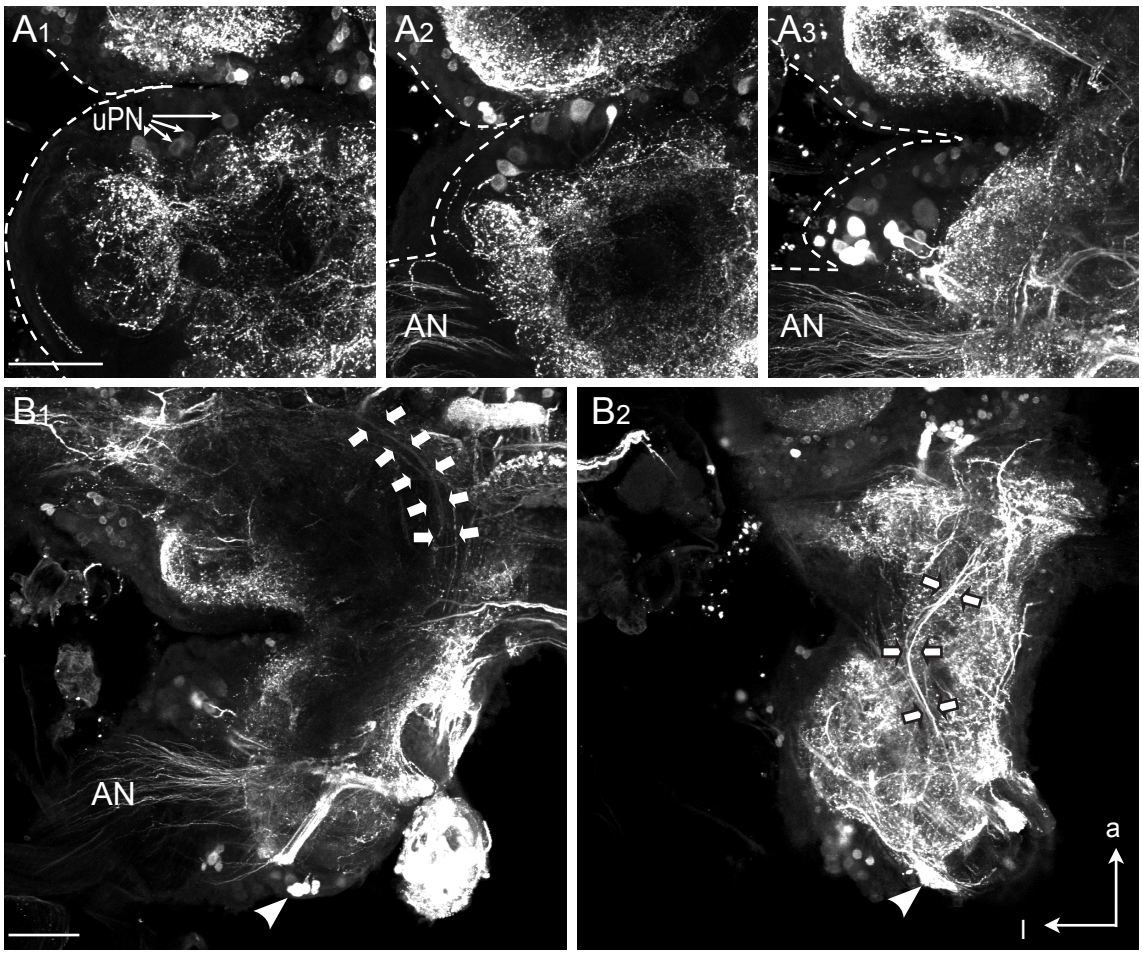

Figure 3.11. Distribution of AST-A-LIR in the AL. A, Overview of AST-A-LIR in the ventral (A_1), medial (A_2) and dorsal (A_3) region of the AL. A_1, weak AST-A-LIR was observed in the uPN soma group and scattered in the region of LN I and LN II somata ($A_{2,3}$). A_3, Strong AST-A-LIR was expressed in a group of somata anterior to the AN. **B**, the iACT (B_1, arrows) was weakly, the ACT IV (B_2, arrows) was stronly AST-A-lir. Note also the prominent ir cluster at the posterodorsal rim of the AL ($B_{1,2}$, arrowhead). Scalebars: 100 µm

Myoinhibitory peptides

A large number of MIP-lir somata ($\sim$ 30 - 50) could be detected in the VSG, of which 2 - 3 could be assigned to the LN I cluster (Fig. 3.12 A_2) and 2 were predicted as LN IIb by the size and location of the somata as well as by the organization of the low order neurites (Fig. 3.12 A_3, see also Fig. 3.1 B). The large majority of immunoreactive somata had a diameter of $\sim$ 20 µm and belonged to a moderately stained cluster, located dorsoanterior of the AL (Fig. 3.12 A_3, B) Neurons of this cluster could not be reliably assigned to either LN I or LN II.
Additional MIP-LIR was found in the posterodorsal soma cluster, that was also AST-A-lir.

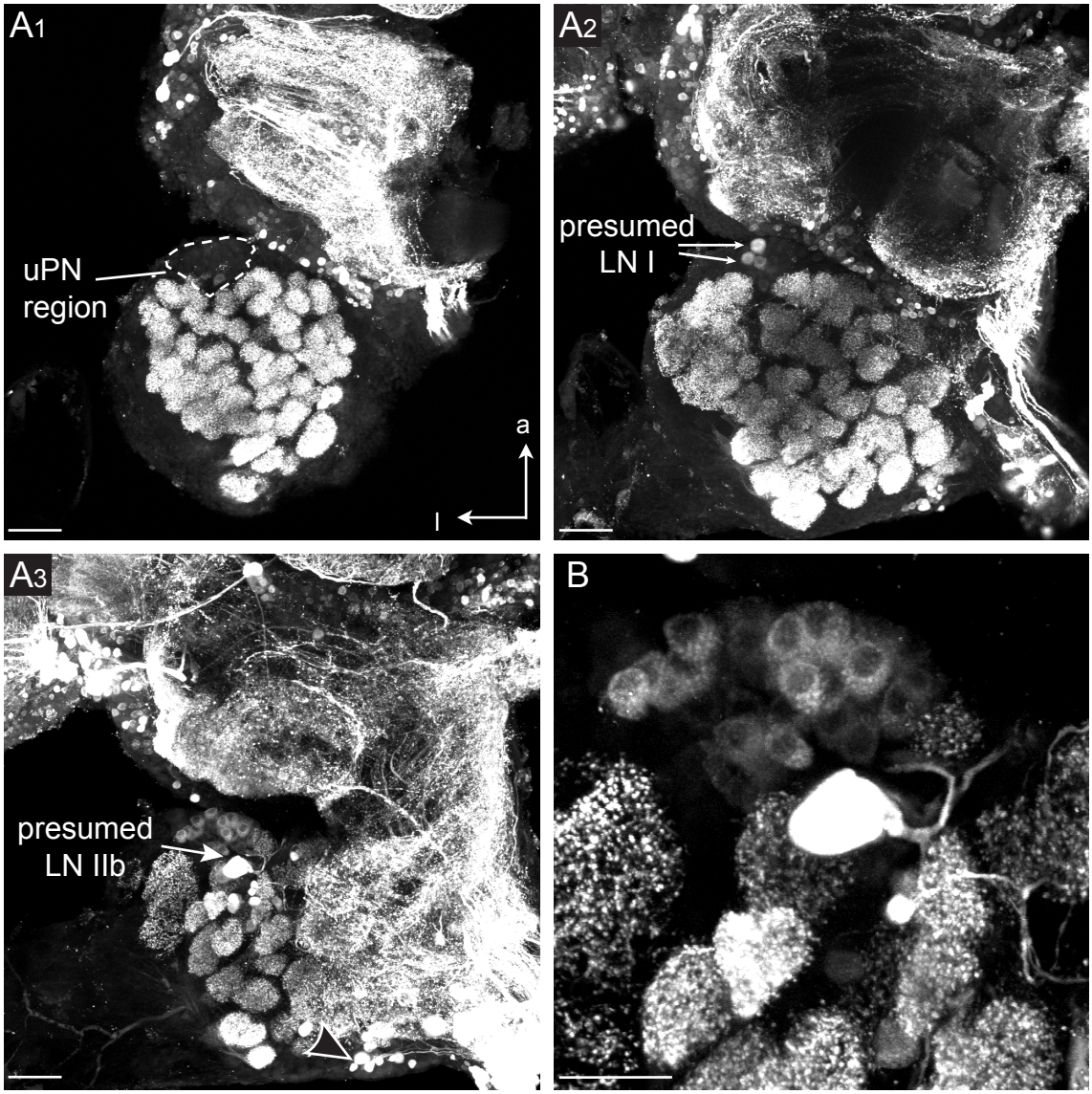

Figure 3.12. Distribution of MIP-LIR in the AL. A, Overview of MIP-LIR in the ventral (A_1), medial (A_2) and dorsal (A_3) region of the AL. A_1, No staining was observed in the uPN soma group. MIP-LIR was expressed in 3 somata in the region of LN I somata (A_2) and in a soma of a putative type IIb LN (A_3). Note also the prominent immunoreactive cluster at the posterodorsal rim of the AL (A_3, arrowhead). **B**, Detailed view of the soma region in A_3 showing a moderately stained soma group anterior to the LN II region. Scale bars: A, 100 µm; B, 50 µm

3.3.2 AT-like imunoreactivity in spiking LN I

5 type I LNs were identified by their morphological and intrinsic electrophysiological properties and then tested for AT-LIR. 60 % (3/5) of the tested LN I were positive for AT (Fig. 3.13). Additionally I analyzed 40 µm vibratome sections of brain preparations that were incubated in antibodies against GABA and AT (Fig. 3.14). The GABA-lir cluster within the VSG can be assumed to exclusively contain somata of GABAergic spiking type I LNs, thus colocalization analysis of GABA- and AT-LIR in the VSG reflects the rate of AT positive LN I. Nearly all (96 %) of the AT-lir somata in the VSG are also immunoreactive for GABA and thus are most likely spiking LN I. In all preparations a distinct subcluster of the GABA-lir LN I somata group colocalizes AT-LIR. 70 $\pm$ 4.6 % (n=4) of the GABA-lir somata are immunoreactive for AT, which is in good agreement with the rate of AT-lir LN I revealed by experiments in single identified interneurons.

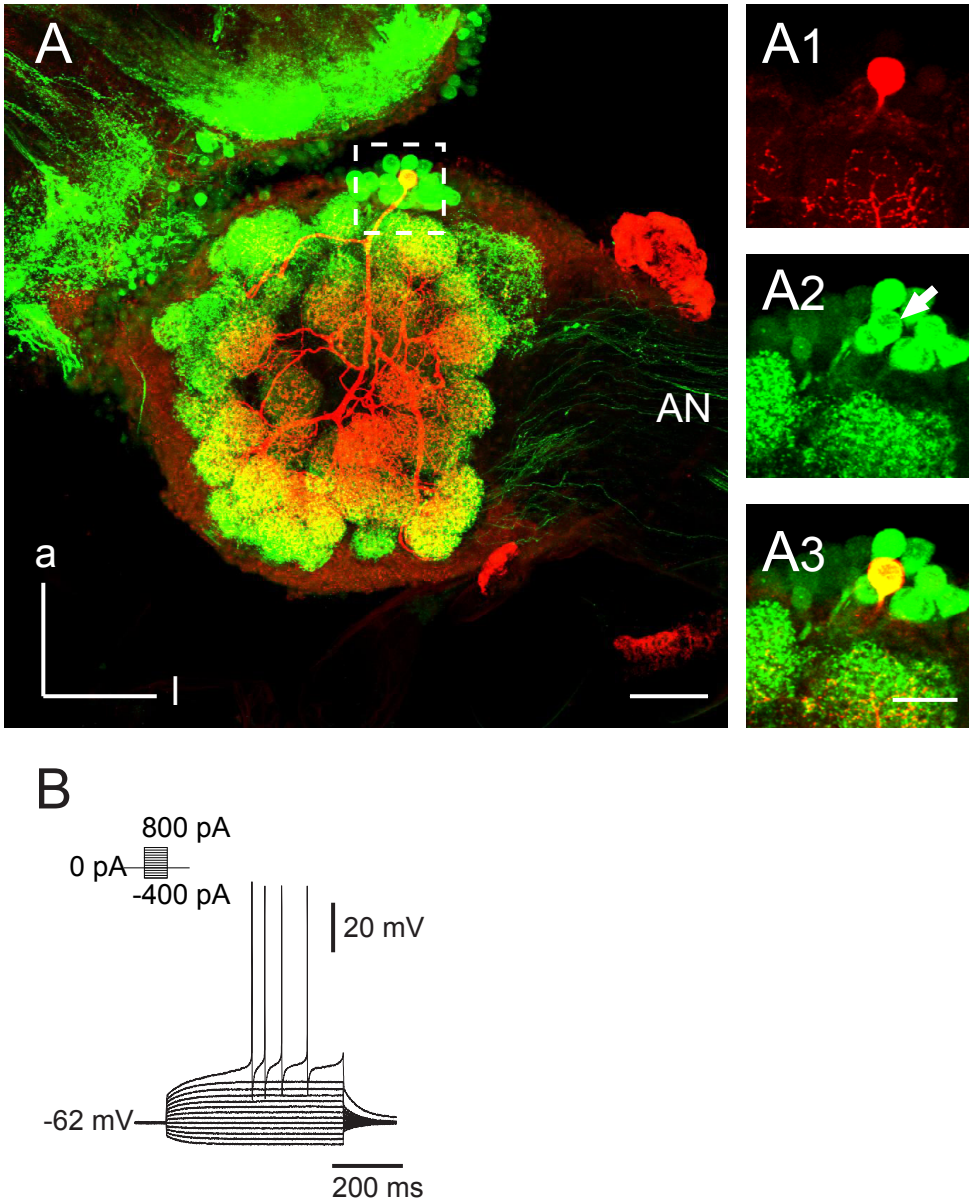

Figure 3.13. AT-lir is expressed in spiking LN I A type I LN was labeled with biocytin/streptavidin (**A_1**, red) and tested for AT-LIR (**A_2**, green). Doublelabeling (**A_3**, yellow) was detected in the soma thus the neuron exhibited AT-LIR. (**B**), current injection evoked for LN I typical Na^+ driven action potentials. Scalebars: A, 100 µm; $A_{1\text{-}3}$, 50 µm

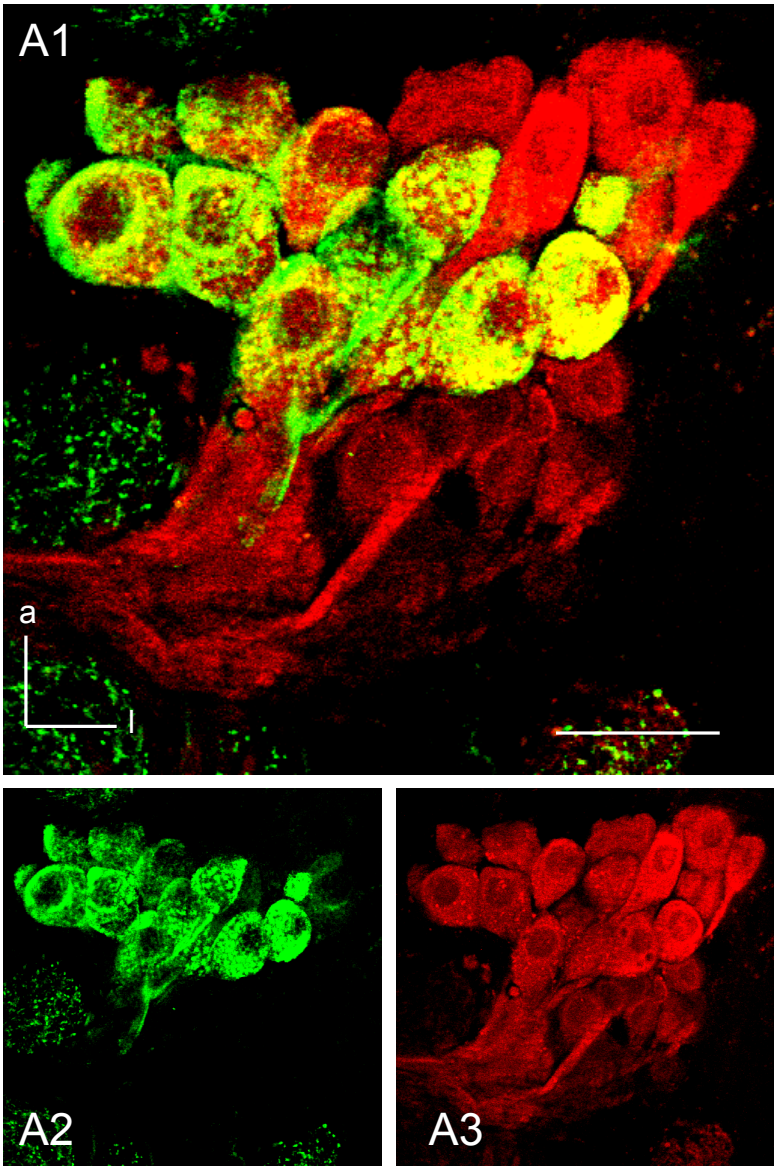

Figure 3.14. A subcluster of the GABA-lir somata group expresses AT-LIR. A section of a 40 µm brain slice displaying the VSG region of the AL was tested for AT-LIR (green) and GABA-LIR (red). **A_1,** merged channels, **A_2,** AT-LIR, **A_3,** GABA-LIR. Colocalization is indicated by doublelabeling (yellow). AT-lir somata ($A_{1,2}$) form a distinct subcluster of the GABA-lir cluster (A_2). Scalebar: 50 µm

3.3.3 TKRP-like imunoreactivity in spiking LN I and nonspiking LN IIa

Wholemount preparations that were stained for anti-TKRP indicate a subcluster of the GABAergic spiking LN I to be TKRP-lir (see Fig. 3.10). Double-labeling against TKRP and GABA in 40 µm vibratome sections indeed shows that 83 ± 0.1 % (n=4) of the TKRP-lir somata in the VSG are also GABA-lir and thus, likely belong to the GABAergic LN I cluster (Fig. 3.15, A), while 17 % do not coexpress GABA-LIR (Fig. 3.15, B).These neurons are potentially nonspiking LN II. 43± 4.1 % of the GABA-lir presumed LN I colocalize TKRP-LIR.

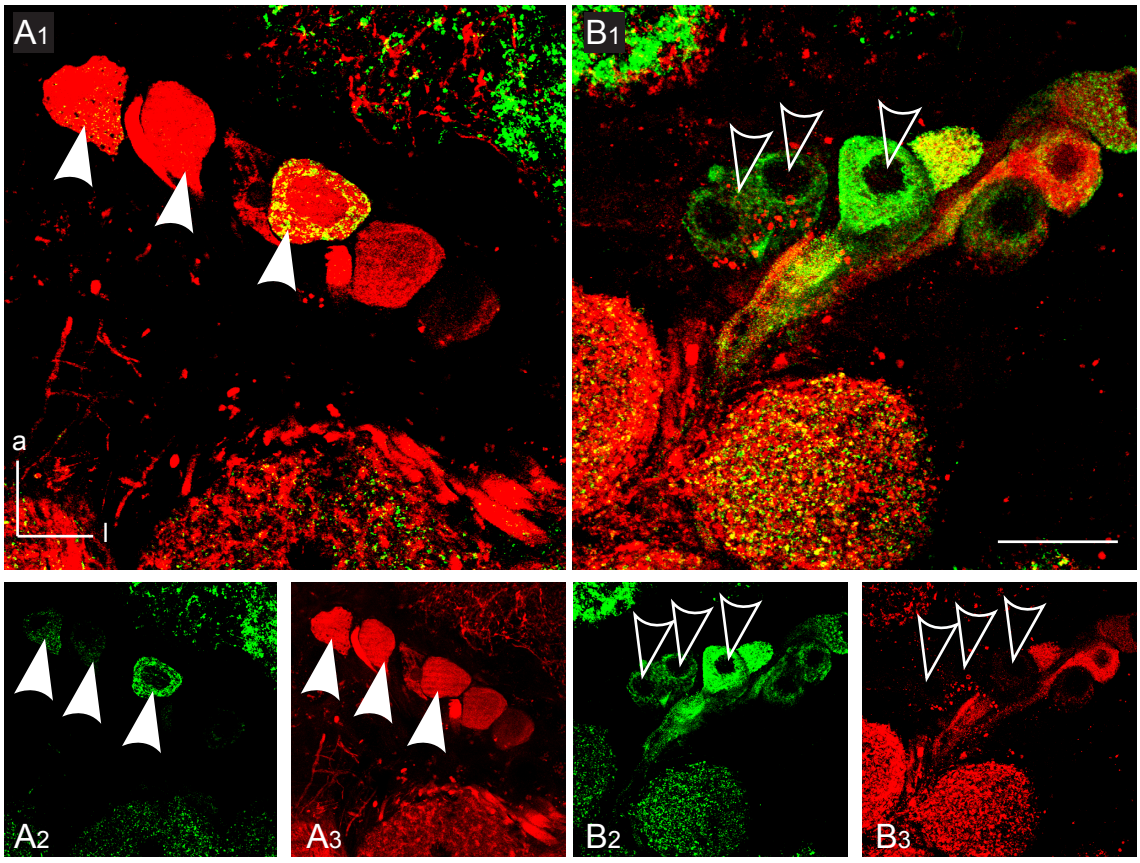

Figure 3.15. TKRP-LIR is expressed in GABA positive and GABA negative somata of the VSG. A, B, Section of consecutive 40 µm brain slices displaying the VSG region of the AL that was tested for TKRP-LIR (green) and GABA-LIR (red) (A,B_1: merged channels, A,B_2: TKRP-LIR, A,B_3: GABA-LIR). Colocalization is indicated by double-labeling (yellow). Many TKRP-lir somata ($A_{1,2}$, filled arrowheads) colocalize GABA-LIR ($A_{1,3}$, filled arrowheads). In a more dorsal region of the VSG some TKRP-lir somata ($B_{1,2}$, open arrowheads) do not express GABA-LIR ($B_{1,2}$, open arrowheads). Scalebar: 50 µm

To verify and specify these assignments I identified 5 LN I and 13 LN II (11 LN IIa, 2 LN IIb) by their morphological and intrinsic electrophysiological properties and then tested them for TKRP-LIR. 2 out of 5 tested spiking LN I expressed TKRP-LIR (40 %), reflecting the results from anti-TKRP/anti-GABA doublelabeling experiments.
72 % of the LN IIa (8/11) and both LN IIb expressed TKRP-LIR. Interestingly all LN IIa_1 (Fig. 3.16) that reacted to an odor stimulus with Ca^{2+} driven spikelets were also TKRP-lir (n=4), while only 57 % (4/7) of the tested LN IIa_2 were TKRP-lir.

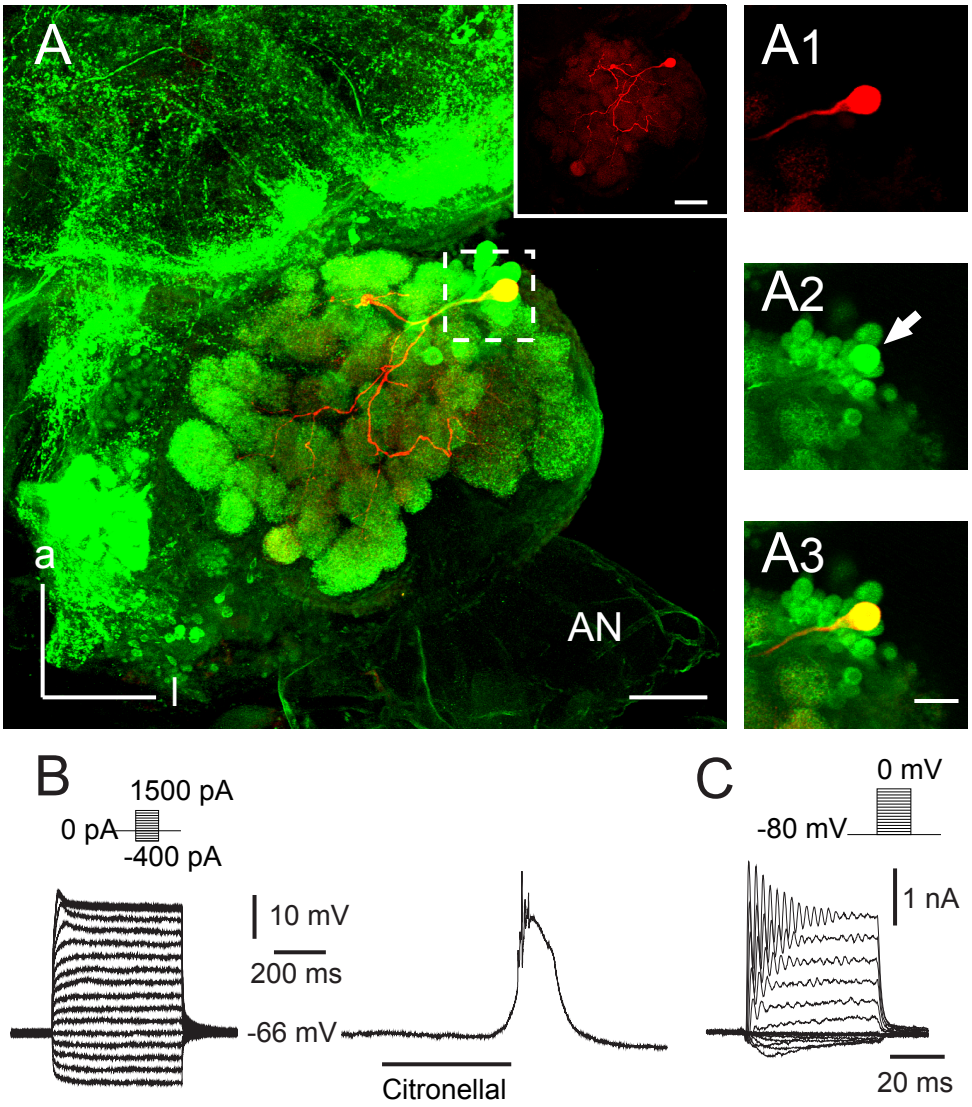

Figure 3.16. TKRP-LIR is expressed in a subgroup of nonspiking LN IIaA type IIa_1 LN was labeled with biocytin/streptavidin (**A_1**, red) and tested for AT-LIR (**A_2**, green). Double labeling (**A_3**, yellow) was detected in the soma thus the neuron exhibited TKRP-LIR. **B**, neither current injection nor odor stimulation evoked Na^+ driven action potentials. The neuron reacted with for LN IIa_1 typical Ca^{2+} spikelets. **C**, Depolarizing voltage steps evoked Ca^{2+} inward and K^+ outward currents, but no transient Na^+ inward currents. Scalebars: A, 100 µm; $A_{1\text{-}3}$, 50 µm

3.4 A method to combine patch clamp recording and single cell staining with single cell MALDI-TOF mass spectrometry

A neuron's computational capacity, and role in a neuronal circuit is determined by its cellular parameters such as morphology, intrinsic electrophysiological characteristics, synaptic properties, and the neurotransmitters or -modulators that they contain and release. To build-up a data set of an individual neuron as complete as possible several approaches like electrophysiology, cell labeling, immunocytochemistry or mass spectrometry have to be combined. Intracellular recordings have been routinely combined with single cell labeling and immunocytochemistry in order to get information on the content of putative neuroactive substances from identified neurons. This technique, however, is limited to known molecules that can be detected by suitable antibodies. Furthermore it is not suitable to investigate a heterogeneous neuronal population or a scattered distribution of multiple neuronal messengers throughout a neuron group.
To attain a complete profiling of neuroactive substances used by antennal lobe interneurons a method was developed that combines patch-clamp recordings and single cell stainings with Matrix-assisted laser desorption/ionization-time of flight mass spectrometry (MALDI-TOF MS).
This work was done in collaboration with Susanne Neupert and Axel Kersting of Reinhard Predel's group.

3.4.1 Methodical approach

The main goal of this study was to establish an experimental approach which provides electrophysiological, morphological, and neurochemical data. Accordingly we combined perforated patch-clamp recordings, dye labeling by single cell electroporation, and single cell MALDI-TOF MS.
In the first set of experiments, I performed whole cell patch clamp recordings prior to mass spectromety. While 86 % of the experiments yielded usable mass

spectra when recorded for a few minutes in whole cell configuration prior to MALDI-TOF MS (< 5 min, n=7), success rate was drastically reduced to 35 % when whole cell recordings were prolonged to 20 - 40 min (n=17).
Since these experiments demonstrated, that the whole cell configuration resulted in a time dependent loss of signals in mass spectra, the perforated patch configuration with gramicidin as a ionophore was used in subsequent experiments. Because cell impermeant dyes or tracer like biocytin are not able to diffuse through the pores built by gramicidin, investigated neurons were juxtasomal labeled by single cell electroporation. The general approach, that comprises three steps, is depicted in figure 3.18.

1. The recording pipette was backfilled with intracellular solution containing biocytin and the ionophore gramicidin. When a tight seal between recording pipette and cell membrane was reached (on cell configuration), the hydrophilic biocytin was loaded into the cell by electroporating stimuli. For this purpose a sequence of 5 - 10 pulse trains of -1 V square pulses with a frequency of 200 Hz and a duration of 500 ms was applied with an interstimulus interval of 5 s (Fig. 3.18 B). There was no evidence that gramicidin, which is lipophilic, crossed the membrane during electroporation. In 79 % of the small diameter uPN somata (11/14) and 57 % of the large diameter LN somata (12/21), the membrane stayed intact after the application of electroporating pulse trains. Biocytin loading via electroporation was successful in 61 % of the experiments (14/23).

2. When the perforated patch configuration was established, hyper- and depolarizing currents were injected and spontaneous activity or rather synaptic input was recorded over 10 to 30 min to electrophysiologically identify the recorded neuron type (Fig. 3.18 C).

3. Ultimately the recording pipette was cautiously withdrawn while pulling a membrane filament from the tip of the pipette, and the soma was then separated from the brain tissue with a wide tip diameter collecting pipette filled with clear saline and immediately placed on a sample plate for MALDI-TOF

ms (Fig. 3.18 D). In the process the intact soma had to be ingested to or into the tip of the collecting pipette by constantly applying gentle negative pressure, thereby cautiously moving the pipette in z (up/down) and y direction (sidewards) to loosen the soma and finally withdrawing the pipette with the attached soma. Results were best when choosing a collecting pipette with a tip diameter of about 1/3 of the respective soma size ($\sim$ 5 - 25 µm).

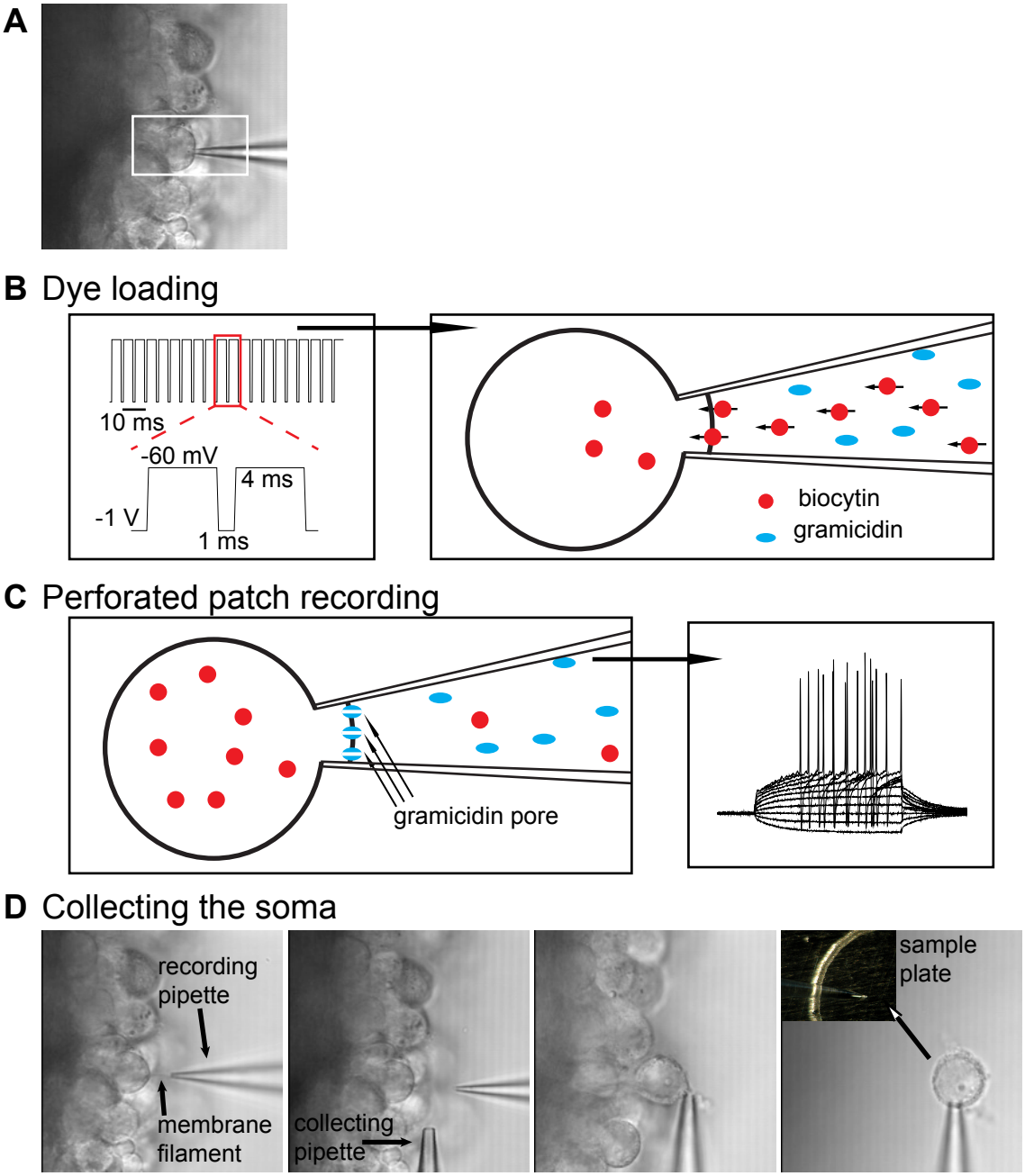

Figure 3.17. A method to combine patch clamp recording and single cell staining with MALDI-TOF MS. A, recording situation in situ. The inset marks a section, that is cartoonized in B and C. **B**, In on cell configuration, a high frequency, high voltage pulse train (left) was used to load the neuron with biocytin by electroporation (right). The lipophilic gramicidin did not cross the membrane. **C**, gramicidin built pores in the membrane, permeable for monovalent cations (left) which allowed to current clamp recordings in perforated patch mode (right). **D**, To collect the soma, the recording pipette was slowly retracted, thereby a membrane filament was carefully pulled from the tip of the pipette. Using a wide tip diameter collecting pipette, the soma was separated from the tissue and placed on a sample plate for subsequent MALDI-TOF MS (left to right).

3.4.2 Validation of the method

The reliability of the method was tested on the homogeneous group of uPNs that send their axons through the iACT. These neurons were shown to express ChAT-LIR thus are likely cholinergic (chapter 3.2.4, Fig. 3.8). Additionally, in the iACT AST-A-LIR is weakly expressed which indicates that uPNs whose axons form the iACT can contain the neuropeptide AST-A (Neupert *et al.* 2012; see also chapter 3.3.1, Fig. 3.11).

7 uPNs were identified by their morphological and physiological properties (Fig. 3.19 A, B) and subsequently collected the for single cell MALDI-TOF MS. In all resulting mass spectra ACh could be detected (Fig. 3.19 C, upper panel). Two spectra showed additional small AST-A signals (Fig. 3.19 C, lower panel).

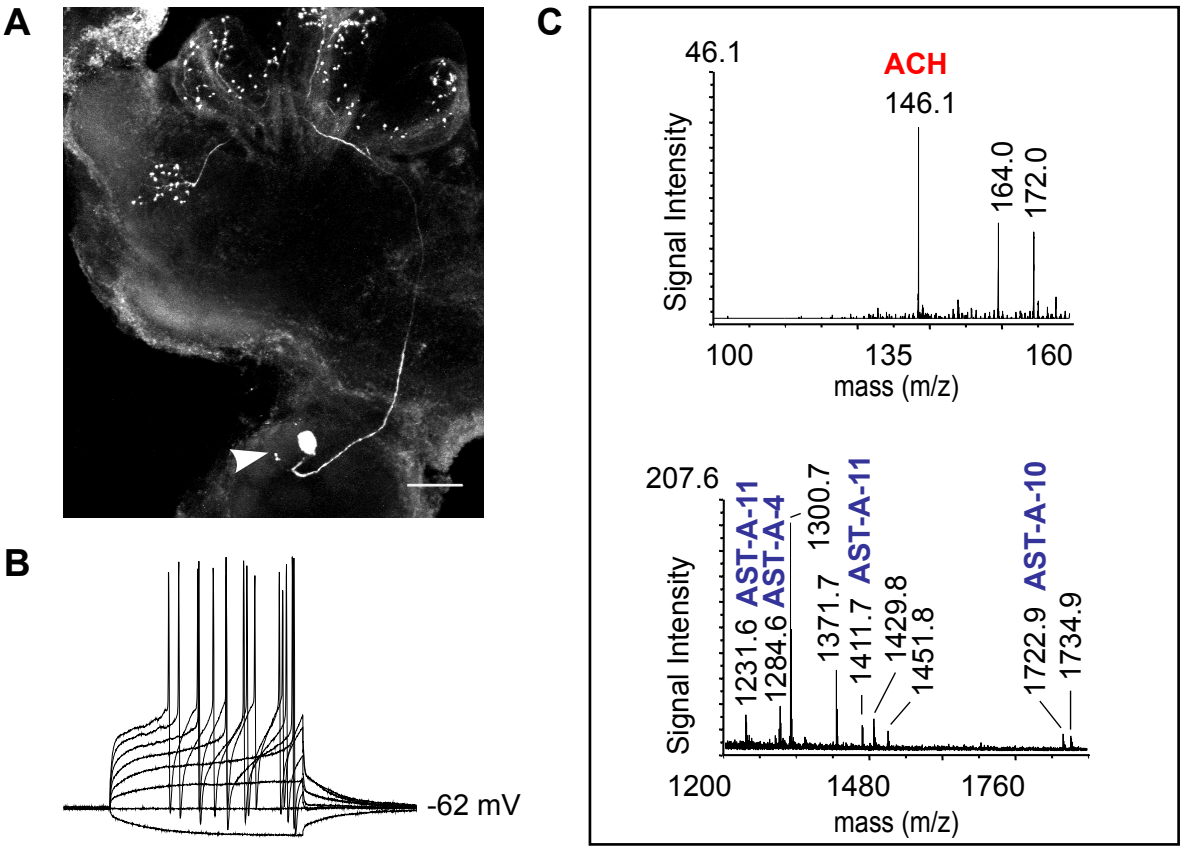

Figure 3.18. ACh and AST-A is expressed in uPNs. A, a uPN was juxtasomal filled and labeled with biocytin/streptavidin (left). The soma (location indicated by the arrowhead) was taken out for MALDI-TOF ms. **B**, current injection evoked for uPNs typical Na^+ driven action potentials. **C**, the resultig mass spectrum revealed ACh (upper spectrum) and AST-A (lower spectrum) to be present in the soma. Scalebar: 100 µm
(mass spectra by Susanne Neupert)

4 Discussion

Although many studies have shown that LNs play an important role for olfactory information processing in insects (Sachse & Galizia, 2002; Stopfer *et al.* , 1997; Tanaka *et al.* , 2009; Wilson & Laurent, 2005; Wilson *et al.* , 2004), the possibility that distinct LN subtypes perform different tasks during olfactory processing has not been explored in detail. Onely recently in the AL of *P. americana* two main LN types with distinct physiological properties (Husch *et al.* , 2009a,b) were characterized: 1) type I LNs that generated Na^+ driven action potentials on odor stimulation and 2) type II LNs, subdivided into IIa and IIb, that did not express voltage dependent transient Na^+ currents and accordingly did not fire action potentials but presumably depend on graded transmitter release.

Previous immunocytochemical and mass spectrometric studies have shown that AL neurons can contain a variety of potential transmitters and neuromodulators Loesel & Homberg, 1999; Nässel & Winther, 2010, reviewed in Homberg, 2002, 1999a). These studies also suggested that classical transmitters might colocalize with potential neuromodulators such as biogenic amines (Dacks *et al.* , 2005, 2006, 2009; Ignell, 2001; Sachse *et al.* , 2006) and peptides (Berg *et al.* , 2006; Nassel & Homberg, 2006; Nässel & Winther, 2010; Utz *et al.* , 2007). To precisely understand the physiological role of potential transmitters and neuromodulators in the AL, it is essential to match the different AL neuron types with their biochemical profiles by combining electrophysiological recordings with immunohistochemical studies and/or single cell mass spectrometry. The marked physiological differences between LN types imply direct consequences for their computational capacity and synaptic output kinetics, and thus their functional role in the olfactory circuit.

4.1 Cholinergic olfactory interneurons

4.1.1 ChAT-lir local Interneurons

This study is based on the previous classification of LNs in the *P. americana* AL by physiological and morphological criteria: spiking LN I, to which I could assign the inhibitory transmitter GABA, and the physiologically distinctive nonspiking LN IIa and LN IIb, that did not express GABA.
With this previous work as a starting point I characterized morphological features and ChAT-LIR for the different LN II subtypes. Type IIa and IIb LNs differed in neurite size and while ChAT-LIR was never found in LN IIb, ∼30% of LN IIa were ChAT-lir. A finer scale analysis revealed two subclasses of type IIa LNs (type IIa1 and type IIa2). These neurons have distinct morphological and physiological features, and engage different transmitters for signaling. Type IIa1 LNs exhibited ChAT-LIR, generated Ca^{2+} driven spikelets and, compared to type IIa2 LNs, had distinct morphological features such as smaller somata and thicker low order neurites. In contrast, type IIa2 LNs did not exhibit ChAT-LIR and did not generate Ca^{2+} driven spikelets.

The strong active membrane properties of type IIa1 LNs, including the ability to generate Ca^{2+} driven spikelets, as well as the larger diameter of neurites, might mediate and facilitate signal propagation to multiple LN IIa1 innervated glomeruli. Thus, type IIa1 LNs might play a similar role as cholinergic LNs in the Drosophila AL that are known to mediate excitatory interglomerular communication (Olsen *et al.* , 2007; Root *et al.* , 2007; Shang *et al.* , 2007; Chou *et al.* , 2010; Das *et al.* , 2008; Huang *et al.* , 2010; Seki *et al.* , 2010; Silbering & Galizia, 2007). The functional relevance of excitatory interactions between the glomerular pathways for structuring the olfactory representation in the AL and regulating the tuning profiles of the PNs has convincingly been shown by physiological studies in the Drosophila AL (Bhandawat *et al.* , 2007; Huang *et al.* , 2010; Olsen *et al.* , 2007; Seki *et al.* , 2010). However, immunocytochemical studies suggested that only few LNs are cholinergic in the Drosophila AL (Chou *et al.* , 2010). This is consistent with

the present study showing that a small subset of LNs expresses ChAT-LIR and thus is most likely cholinergic. This study supports and extends previous results (Husch *et al.* , 2009a) and clearly identifies GABA as the transmitter of spiking type I LNs whereas ACh serves as the transmitter of nonspiking type IIa1 LNs.

4.1.2 ChAT-lir projection neurons.

Applying immunocytochemical staining and, for the first time, immunocytochemistry combined with single labeling and elctrophysiological characterization, I could show that the uPNs with somata in the ventral VSG and projections in the iACT are cholinergic. This is consistent with previous immunocytochemical studies in several insect species including *D. melanogaster, M. sexta, A. mellifera* and *S. gregaria* which suggested that uPNs might be cholinergic (Buchner *et al.* , 1986; Homberg, 2002; Homberg *et al.* , 1995; Bicker, 1999; Gorczyca & Hall, 1987; Kreissl & Bicker, 1989; Scheidler *et al.* , 1990; Yasuyama *et al.* , 2003). However, the transmitters of other PN types still need to be identified. In *P. americana* as in many other insects the AL is connected to the protocerebrum by different types of PNs. They can, for example, be multiglomerular (Abel *et al.* , 2001; Kanzaki *et al.* , 1989; Lai *et al.* , 2008; Rössler & Zube, 2011) and, depending on the species, they can give rise to different tracts (Galizia & Rössler, 2010; Malun *et al.* , 1993).

4.1.3 Western blotting

While previous reports on the size of native *Drosophila* ChAT (dChAT) could be conflicting, the calculated molecular weight of the deduced amino acid sequence from the cDNA is 81 kDa, and Western blots using two different dChAT antibodies showed bands at about that particular molecular weight (Itoh *et al.* , 1986; Sugihara *et al.* , 1990; Takagawa & Salvaterra, 1996). Here, the ChAT4B1 antibody marked a corresponding band at ∼80 kDa in all *Drosophila* and *Periplaneta* samples, thus it is reasonable that this band represents a dChAT-like protein. In some cases the major bands corresponding to the ChAT protein were accompanied by less prominent bands at ∼65 kDa, 55 kDa and 45 kDa in samples of *P. americana*

AL homogenates and at ∼65 kDa and 60 kDa in samples of crude fly head homogenates respectively.
Studies on *Drosophila*ChAT demonstrated that a purified dChAT sample showed major bands at 67 kDa and 54 kDa in SDS-PAGE which were both stained in Western blotting using the ChAT1G4 antibody (Slemmon *et al.* , 1982; Salvaterra & McCaman, 1985). These proteins were considered degradation products.

4.2 Peptidergic olfactory interneurons

Immunocytochemical studies in various insects suggest, that olfactory neurons express a large variety of putative neurotransmitters and modulators, including neuropeptides, that can also colocalize other peptides or classical transmitters (reviewed in Homberg, 1999a; Nassel & Homberg, 2006; Utz *et al.* , 2007; Nässel & Winther, 2010). An approach to understand the physiological role of neuropeptides in the AL is to match the functionally different cell types with their peptide profiles. To gain an understanding of the peptides functional role in the AL, I explored their expression pattern in distinct AL neuron types and unequivocally assigned allatotropin to a subpopulation of GABAergic LN I and tachykinin-related peptides to both subpopulations of LN I and cholinergic LN IIa1, by using a combination of electrophysiological recordings and immunocytochemical studies.

4.2.1 Neuropeptides in distinct AL soma clusters

Allatotropin

My studies on the expression of AT revealed the majority of AT-lir somata in the AL to belong to the spiking LN I, that were also shown to be GABA-lir (Husch *et al.* , 2009a). In addition, colocalization of AT-LIR and GABA-LIR was demonstrated in the VSG somata which strongly indicates, that AT and GABA are coexpressed in a subpopulation of spiking LN I.

Allatotropins are highly conserved in insects. Members of the AT family have

been identified in various insect species (summarized in Homberg *et al.* , 2004). The cockroach AT was recently identified from *P. americana* (Neupert *et al.* , 2009) and mass spectra of different AL soma clusters confirmed the presence of *at*-gene products in the AL (Neupert *et al.* , 2012). Immunocytochemical studies on the distribution of AT in the insect brain revealed similar staining patterns in all investigated species including the cockroach *L. maderae* (Homberg, 1999b). In all cases AT-LIR was demonstrated in a set of LNs that innervate all glomeruli and often co-localized GABA and other peptides (reviewed in Schachtner *et al.* , 2005; Nassel & Homberg, 2006), which is in agreement with the present study. However, little is known about the physiological relevance of AT expression in these neurons. In the abdominal nervous system of the cockroaches *L. maderae* and *P. americana Manduca sexta*-AT (Mas-AT) increased the heart beat of the abdominal hearts (positive chronotropic response) and in the *L. maderae* hindgut, Mas-AT increased the frequency of spontaneous contraction (Rudwall *et al.* , 2000). Horodyski *et al.* (2011) demonstrated that activation of a Mas-AT receptor expressed in HEK293 cells results in an increase in cAMP levels which indicates, that AT may act through a G-protein coupled second messenger pathway.

Tachykinin-related peptides

In the AL of *P. americana*, I demonstrated clustered TKRP-LIR in GABA-lir VSG somata as well as in GABA-negative VSG somata. On the single cell level, I confirmed a subpopulation of spiking LN I, that were shown to express GABA-LIR (Husch *et al.* , 2009a), to be TKRP-lir and most, if not all LN IIa1, that were shown to be ChAT-lir (see chapter 4.1 Cholinergic olfactory interneurons), to express TKRP-LIR. These findings suggest, that TKRPs are coexpressed with GABA in LN I and with ACh in LN IIa1.

TKRPs form a well conserved family of multifunctional brain/gut peptides across phyla (Lundquist & Nässel, 1997; Nässel, 1999; Otsuka & Yoshioka, 1993; Vanden Broeck *et al.* , 1999). The TKRP precursor sequence of *P. americana* contains

13 copies of related TKRPs, that where biochemically identified in the CNS and detected in mass spectra of AL glomeruli and distinct AL soma cluster (Predel *et al.* , 2005; Neupert *et al.* , 2012). Mass spectrometrical and immunocytochemical studies in several insect species demonstrated the abundance of TKRP expressing neurons in the olfactory system (reviewed in Nässel & Winther, 2010; Nässel, 1999). While TKRP-LIR was always colocalized with GABA-LIR in AL LNs of *L. maderae* (Nässel *et al.* , 2000) and *S. gregaria* (Ignell, 2001), TKRP-lir LNs in the AL of *H. virescens* did not colocalize GABA-LIR (Berg *et al.* , 2009).
While invertebrate TKRPs have been identified and isolated extensively in several species, only five corresponding G protein coupled receptors have been properly characterized so far (summarized in Van Loy *et al.* , 2010). In the fruit fly, prominent presence of a TKRP receptor was detected in several neuropilar structures of the brain including the ALs (Birse *et al.* , 2006). Recent studies in *Drosophila* revealed that this receptor, designated DTKR, is expressed both in OSNs, were the *Drosophila* tachykinin 1 (DTK1) suppresses presynaptic calcium and synaptic transmission, and in LNs, that partly also express the ligand, hence it was suggested that the peptidergic LNs may signal not only to OSNs but also to each other (Ignell *et al.* , 2009; Winther & Ignell, 2010).

Allatostatin A

AST-A could be assigned to uPNs by imunocytochemical and mass spectrometrical methods. Additionally, antibody stainings suggest that one individual, presumably type IIb LN expresses AST-A. Besides the VSG, immunoreactive neurons with processes in the AL were found in a posterodorsal soma cluster. Neurons of this cluster, which are referred to as T-cells (Neupert *et al.* , 2012), have not been described in detail yet. However, preliminary electrophysiological experiments on neurons whose soma size and location match that of the T-cells were carried out (see Appendix). Recorded cells, some of which were successfully stained, generated TTX sensitive action potentials on odor stimulation and current injection (Fig. 5.2). Single cell labeling revealed two main projections,

that probably run through the T-shaped tract (Fig.5.3): An 'ascending' projection to the AL, where several glomeruli were innervated, as well as to the lateral protocerebrum, a diffuse neuropile at the intersection between proto- and deutocerebrum, that is also innervated by thermo- and hygrosensory PNs (Nishino *et al.* , 2003), and an additional 'descending' projection to the *lobus glomeratus* of the tritocerebrum, where axons from the maxillary palps terminate (Ernst *et al.* , 1977). AST-lir somata with a roughly similar location and projection to the deuto- and tritocerebrum were described before in the german cockroach *B. germanica* (Maestro *et al.* , 1998).

The AST-A precursor sequence of *P. americana* contains 14 copies of related AST-A (Reichwald *et al.* , 1994; Ding *et al.* , 1995), most of which were identified in mass spectra of AL glomeruli (Neupert *et al.* , 2012). AST-A-lir fibers originating from LNs, PNs and/or centrifugal neurons have been demonstrated in the ALs of a broad spectrum of insect species (silverfish: Schachtner *et al.* 2005; fly: East *et al.* 1995; bee: Kreissl *et al.* 2010; moth: Berg *et al.* 2007; Utz & Schachtner 2005; Locust: Vitzthum *et al.* 1996), suggesting that AST-A plays a common role in the insect olfactory circuit. Physiological studies on allatostatin action provide evidence, that a cockroach allatostatin (DipAST-1) and crustacean allatostatins inhibit the Mas-AT induced contractions of the posterior hindgut in *L. maderae*, but not spontaneous contractions or contractions induced by other peptides (Dircksen *et al.* , 1999). In the moth foregut AST-A inhibits the Mas-AT stimulation of frequency and amplitude of contractions (Duve *et al.* , 1999). Immunostainings (this study) and mass spectrometrical experiments (Neupert *et al.* , 2012) revealed AST-A to be present along with AT in the glomeruli of the *P. americana* AL. Accordingly, these peptides could potentially act as antagonists in the olfactory circuit.

4.2.2 Peptide cotransmission

AT-LIR and TKRP-LIR were demonstrated to be colocalized with GABA in LN I and TKRP to be coiocalized with ChAT-LIR in LNIIa1. In addition to the clustered peptidergic somata of LN I and LN IIa1, immunocytochemical stainings and mass spectra of AL tissue containing LN II somata suggest the expression of multiple peptides, each in a small number of neurons (for additional peptides see Neupert *et al.* , 2012).

Apparently, it is a common feature of antennal lobe LNs to coexpress different neuropeptides and a classical neurotransmitter such as GABA (Berg *et al.* , 2009; Birse *et al.* , 2006; Ignell *et al.* , 2009; Nassel & Homberg, 2006; Utz *et al.* , 2008), still, the functional role of peptide cotransmission in the insect brain and whether peptides act synergistically with other transmitters or independently has not yet been well explored.

In mammals, as well as in the mollusc *Aplysia californica* it has been found that at synapses where classical neurotransmitters and peptides are colocalized, vesicles containing classical transmitters are stored close to the active zone of the presynaptic membrane whereas the neuropeptide containing vesicles are found in the perisynaptic area (Karhunen *et al.* , 2001; Merighi, 2002; Salio *et al.* , 2006). The distinct location of vesicles containing different messenger classes can have consequences for release dynamics and target area and thus could contribute to synaptic plasticity.

4.3 MALDI-TOF MS in identified interneurons

In collaboration with Reinhard Predel's group, I established an experimental approach which provides electrophysiologal, morphological and neurochemical parameters of single neurons. These experiments involve the mass spectrometric analysis of cytosolic contents of the examined cells. Substances like transmitters or neuropeptides, that are dissolved in the cytosol are rapidly washed out in whole cell configuration, which can diminish or even abolish respective signals

in mass spectra. Accordingly we combined perforated patch-clamp recordings, dye labeling by single cell electroporation and single cell MALDI-TOF mass spectrometry.

We first used this combined approach to test directly if uPNs are cholinergic as shown by immunostaining against the biosynthetic enzyme ChAT. The homogeneity of the uPN population makes them suitable not only to show the feasibility of our combined approach, but also to demonstrate its reliability and reproducibility.

Applying this new approach, we confirmed the expression of ACh in neurons that were electrophysiologically and morphologicaly identified as uPNs. The MALDI-TOF MS analysis revealed very reproducible spectra which clearly contained a distinct ion signal mass that was identical to ACh. This is the first direct evidence for ACh expression in uPNs.

Two uPN mass spectra showed also the presence of AST-A. This is remarkable because in immunocytochemical studies clear AST-A-LIR was only detected in the axonal tracts of uPNs, while only vague AST-A-LIR was detected in the uPN somata (see chapter 3.3.1 figure 3.11).

Single neuron techniques that have been combined successfully and routinely include electrophysiological recordings, dye loading, immunocytochemistry and RT-PCR. However, patch-clamp recordings and MALDI-TOF MS, two utmost powerful electrophysiological or rather (bio)chemical methods, have not been combined routinely on the single cell level before. While patch clamp recordings allow analyzing the cellular electrophysiological properties in great detail, MALDI-TOF MS is extremely effective in identifying simultaneously a multitude of potential neurotransmitters and neuromodulators of different chemical classes. We consider the combination of these techniques a powerful tool to yield unambiguous information about the neurotransmitters and -modulators of unequivocally identified neurons.

4.4 Summary and Conclusion

In this thesis neurotransmitters and -modulators have been assigned to distinct LN subtypes. A summary of physiological, morphological and neurochemical properties of AL neurons is provided in figure 4.1: LN I that responded to odor stimulation with Na^+ driven action potentials were GABA-like immunoreactive, thus inhibitory. Additionally defined subpopulatios, which might also overlap, were immunoreactive for allatotropin and tachykinin-related peptides. Among the group of type IIa LNs Type, I found two subtypes that were morphologically and physiologically distinguishable and expressed different neuronal messengers. LN IIa1 responded to odor stimulation with calcium driven transients and expressed ChAT-like immunoreactivity, thus they were likely cholinergic and excitatory. Most type IIa1 LNs were additionally immunoreactive for tachykinin-related peptides. In contrast, LN IIa2 did not elicit calcium transients and did not express ChAT-like immunoreactivity. Low order neurites were finer and the soma was larger compared to type IIa1 LNs. While LN I and LN IIa1can hypothetically trigger synaptic transmitter release by patterns of sodium and calcium transients respectively, which in case of LN IIa1 would likely be restricted to few glomeruli, LN IIa2 and LN IIb only generate graded depolarizations that might spread only within the same gomerulus and result in graded transmitter- or modulator release for intra- rather than interglomerular communication.

To fully understand the functional role of distinct LNs in the olfactory network, it is important to determine the input- and output-sites of each LN subtype and with which cell types they form synapses. Though electron microscopical data is available in the cockroach (Distler & Boeckh, 1997a,b; Distler *et al.* , 1998), cholinergic and peptidergic local interneurons were not concidered in these studies. Further, electrophysiological studies on peptide action are needed to determine the physiological relevance of these putative neuroactive substances.

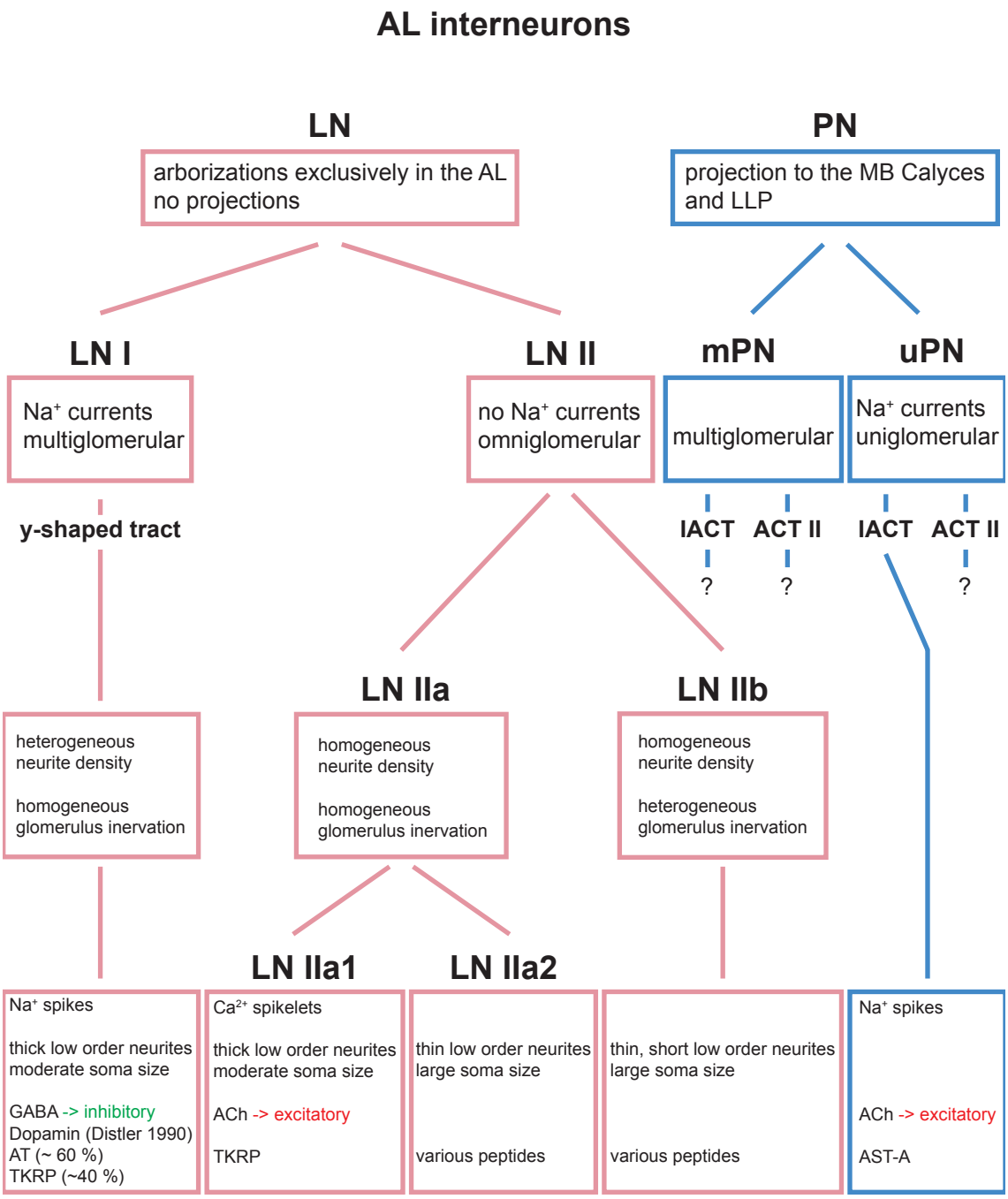

Figure 4.1. Overview of AL interneurons in *P. americana*.

5 Appendix

AST-A-LIR T-cells in a posterodorsal soma cluster of the deutocerebrum.

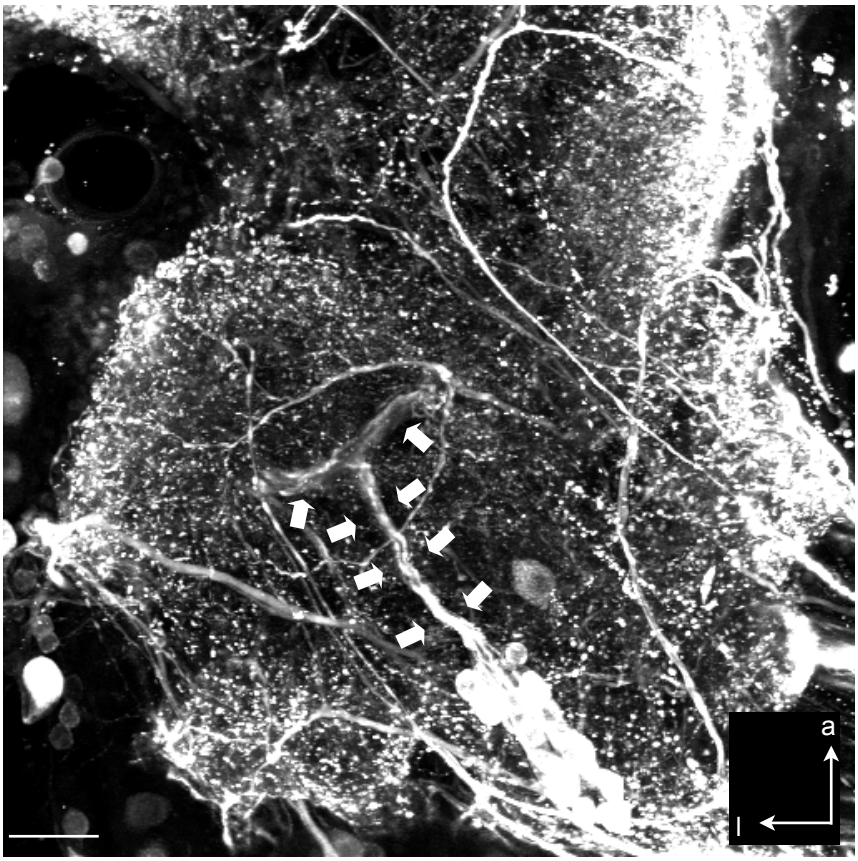

Figure 5.1. AST-A LIR in a posterodorsal soma cluster of the deutocerebrum. Maximum intensity image stack of an anti-AST-A immunostained AL. Besides the VSG strong immunoreactivity was found in a densely packed soma cluster located outside the AL at the posterodorsal rim of the deutocerebrum. The axons of these neurons formed a characteristic T-shaped tract before entering the AL (arrows).

Morphological and electrophysiological characteristics of putative T-cells.

Figure 5.2 *(following page).* Morphological and electrophysiological characteristics of a neuron from the posterodorsal deutocerebrum. A, Morphological details of a single neuron that was labeled with biocytin/streptavidin (white). Neuropils were immunostained with α-synapsin (red). (Left) Reconstruction of the biocytin/streptavidin label showing an overview of arborizations in the antennal lobe and projections to the lateral protocerebrum and the *lobus glomeratus* of the tritocerebrum. The soma, indicated by the asterix, was located at the posterodorsal rim of the deutocerebrum. (Right) Confocal fluorescence images of brain regions indicated by the respective inset in the reconstruction. (1) T-shaped primary neurites. (2) Processes in the lateral protocerebrum. (3) Sparse glomerular innervation in the AL. (4) Projection embracing the LGT. Note that no processes were observed innervating the neuropil of the LGT. **B** Current clamp recording of spontaneous activity. The neuron spontaneously elicited bursts of action potentials in an unsteady frequency. **C** Current clamp recording of responses to stimuli with three different odorants. The neuron responded with odor specific depolarizations that gave rise to overshooting action potentials. **D** Injection of a depolarizing current evoked actionpotentials that were not abolished in cadmium- but in TTX containing saline. Voltage scales apply for all recordings. AL: antennal lobe, LGT: *lobus glomeratus* of the tritocerebrum, PC: protocerebrum, scalebars in (A): 50 µm.

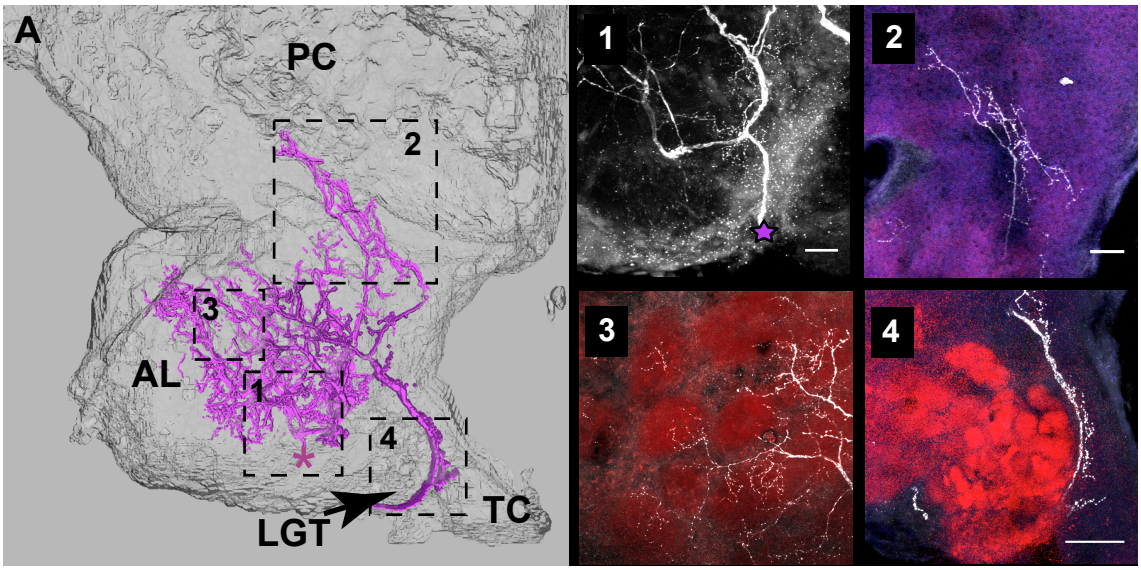
A
PC
2
3
AL
1
4
LGT
TC
1
2
3
4

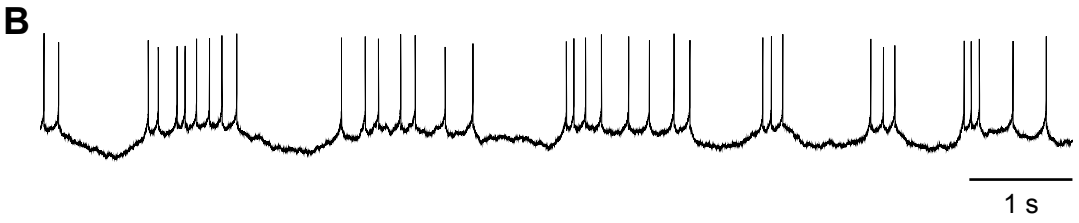
B
1 s

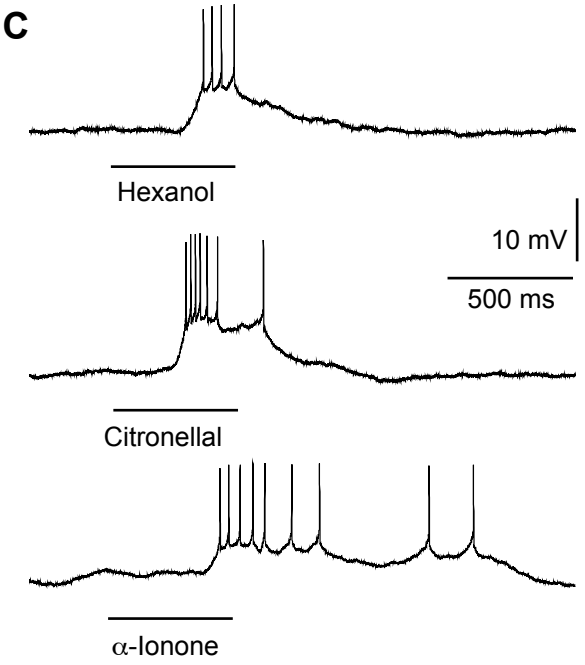
C
Hexanol
10 mV
500 ms
Citronellal
α-Ionone

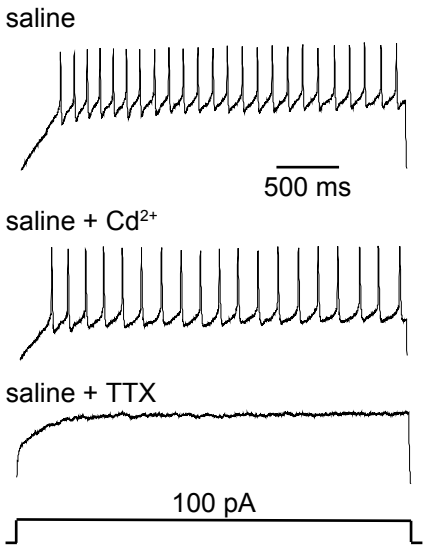
D
saline
500 ms
saline + Cd2+
saline + TTX
100 pA

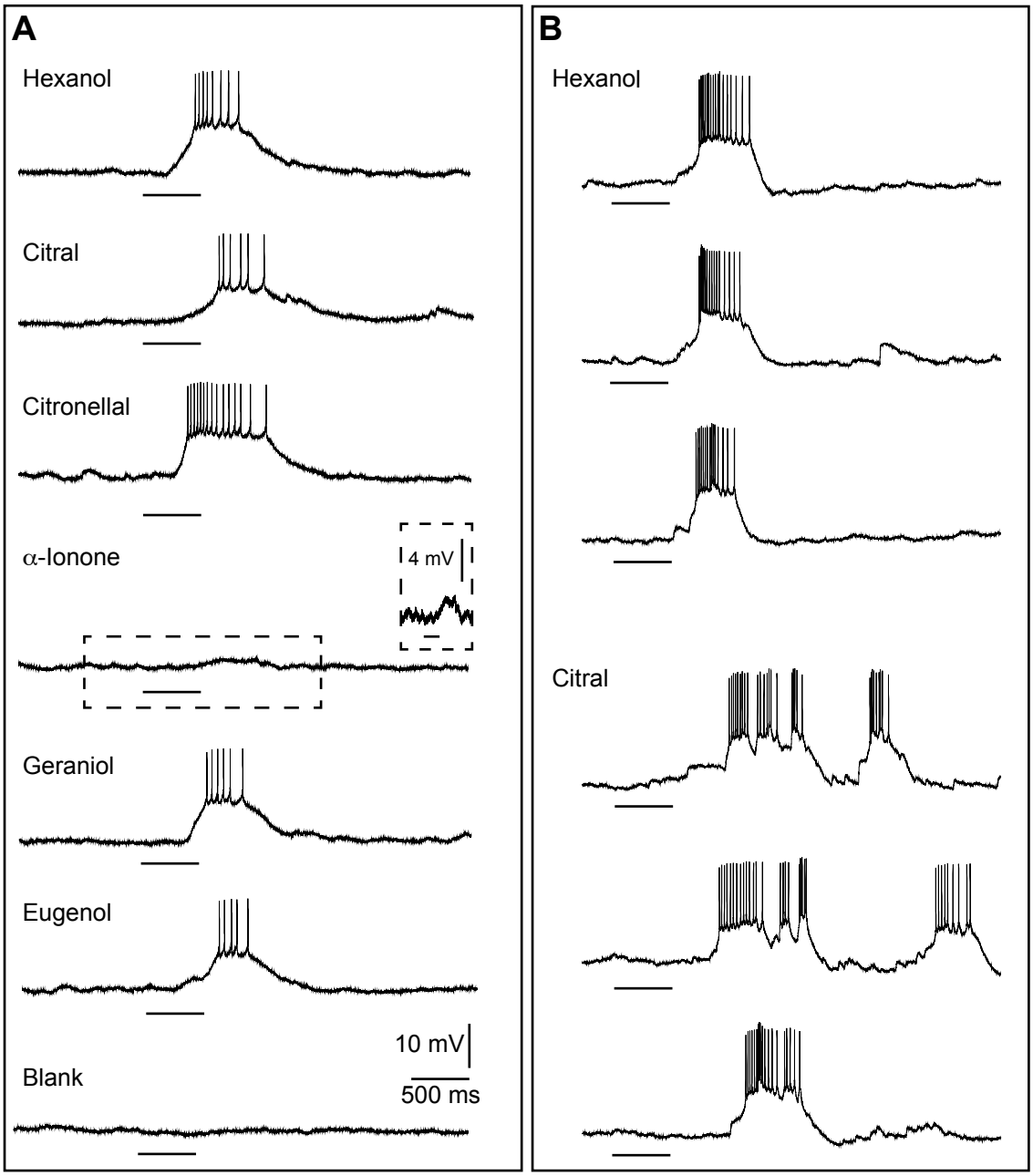

Figure 5.3. Typical responses of neurons from the posterodorsal soma cluster of the deutocerebrum to different odors. Whole cell patch clamp recording during odor stimulation. Six odorants and a blank (mineral oil) were used. The bar beneath the recording indicates the opening of the solenoid valve of the stimulation unit (500 ms). A, Typical odor responses of a neuron from the posterodorsal deutocerebrum. They respond to odorants of many different chemical types, mostly with overshooting action potentials on top of a depolarization. During the blank stimulation no change in membrane potential was recorded. B, Repetitive odor stimulation. Odor stimulation was applied three times with one minute intervals. While the overall spiking pattern is robust, slight variations between trials were detected.

List of Figures

List of Tables

References

ABEL, R., RYBAK, J., & MENZEL, R. 2001. Structure and response patterns of olfactory interneurons in the honeybee, Apis mellifera. *J Comp Neurol*, **437**(3), 363–383.

ADLER, J., PAGAKIS, S. N., & PARMRYD, I. 2008. Replicate-based noise corrected correlation for accurate measurements of colocalization. *J Microsc*, **230**(Pt 1), 121–133.

AKAIKE, N. 1996. Gramicidin perforated patch recording and intracellular chloride activity in excitable cells. *Prog Biophys Mol Biol*, **65**(3), 251–264.

ARMSTRONG, C. M., & BEZANILLA, F. 1974. Charge movement associated with the opening and closing of the activation gates of the Na channels. *J Gen Physiol*, **63**(5), 533–552.

BARLOW, ANDREW L., MACLEOD, ALASDAIR, NOPPEN, SAMUEL, SANDERSON, JEREMY, & GUÉRIN, CHRISTOPHER J. 2010. Colocalization Analysis in Fluorescence Micrographs: Verification of a More Accurate Calculation of Pearson's Correlation Coefficient. *Microscopy and Microanalysis*, **16**(06), 710–724.

BAZENOV, M., STOPFER, M., RABINOVICH, M., ABARBANEL, H. D.I., SEJNOWISK, T. J., & LAURENT, G. 2001. Model of cellular and network mechanisms for odor-evoked temporal patterning in the locust antennal lobe. *Neuron*, **30**(2), 569–81.

BERG, BENTE G, SCHACHTNER, JOACHIM, UTZ, SANDRA, & HOMBERG, UWE. 2007. Distribution of neuropeptides in the primary olfactory center of the heliothine moth Heliothis virescens. *Cell Tissue Res*, **327**(2), 385–398.

BERG, BENTE G., SCHACHTNER, JOACHIM, & HOMBERG, UWE. 2009. Gamma-aminobutyric acid immunostaining in the antennal lobe of the moth Heliothis virescens and its colocalization with neuropeptides. *Cell Tissue Res*, **335**(3), 593–605.

BERG, B.G., SCHACHTNER, J., UTZ, S., & HOMBERG, U. 2006. Distribution of neuropeptides in the primary olfactory center of the heliothine moth Heliothis virescens. *Cell and Tissue Research*, Sep 30.

BHANDAWAT, VIKAS, OLSEN, SHAWN R, GOUWENS, NATHAN W, SCHLIEF, MICHELLE L, & WILSON, RACHEL I. 2007. Sensory processing in the Drosophila antennal lobe increases reliability and separability of ensemble odor representations. *Nat Neurosci*, **10**(11), 1474–1482.

BICKER, G. 1999. Histochemistry of classical neurotransmitters in antennal lobes and mushroom bodies of the honeybee. *Microsc Res Tech*, **45**(3), 174–183.

BIRSE, RYAN T., JOHNSON, ERIK C., TAGHERT, PAUL H., & NÄSSEL, DICK R. 2006. Widely distributed Drosophila G-protein-coupled receptor (CG7887) is activated by endogenous tachykinin-related peptides. *J Neurobiol*, **66**(1), 33–46.

BOECKH, J., & ERNST, K.-D. 1987. Contribution of single unit analysis in insects to an understanding of olfactory function. *Journal of Comparative Physiology A*, **161**, 549–565.

BOECKH, J., & TOLBERT, L. P. 1993. Synaptic organization and development of the antennal lobe in insects. *Microsc Res Tech*, **24**(3), 260–280.

BOECKH, J., ERNST, K.D., SASS, H., & WALDOW, U. 1984. Anatomical and physiological characteristics of individual neurones in the central antennal pathway of insects. *Journal of Insect Physiology*, **30**(1), 15 – 26.

BUCHNER, E, BUCHNER, S, CRAWFORD, G, MASON, WT, SALVATERRA, PM, & SATTELLE, DB. 1986. Choline acetyltransferase-like immunoreactivity in the brain of Drosophila melanogaster. *Cell and Tissue Research*, **246**(1), 57–62.

CHOU, YA-HUI, SPLETTER, MARIA L, YAKSI, EMRE, LEONG, JONATHAN C S, WILSON, RACHEL I, & LUO, LIQUN. 2010. Diversity and wiring variability of olfactory local interneurons in the Drosophila antennal lobe. *Nat Neurosci*, Feb.

CHRISTENSEN, T. A., WALDROP, B. R., HARROW, I. D., & HILDEBRAND, J. G. 1993. Local interneurons and information processing in the olfactory glomeruli of the moth Manduca sexta. *J Comp Physiol A*, **173**(4), 385–399.

DACKS, A. M., CHRISTENSEN, T. A., AGRICOLA, H. J., WOLLWEBER, L., & HILDEBRAND, J. G. 2005. Octopamine-Immunoreactive Neurons in the Brain and Subesophageal Ganglion of the Hawkmoth Manduca sexta. *The Journal of comparative neurology*, **488**(3), 255–68.

DACKS, ANDREW M, CHRISTENSEN, THOMAS A, & HILDEBRAND, JOHN G. 2006. Phylogeny of a serotonin-immunoreactive neuron in the primary olfactory center of the insect brain. *J Comp Neurol*, **498**(6), 727–746.

DACKS, ANDREW M, GREEN, DAVID S, ROOT, CORY M, NIGHORN, ALAN J, & WANG, JING W. 2009. Serotonin modulates olfactory processing in the antennal lobe of Drosophila. *J Neurogenet*, **23**(4), 366–377.

DANIELS, RICHARD W, GELFAND, MARIA V, COLLINS, CATHERINE A, & DIANTONIO, AARON. 2008. Visualizing glutamatergic cell bodies and synapses in Drosophila larval and adult CNS. *J Comp Neurol*, **508**(1), 131–152.

DAS, ABHIJIT, SEN, SONIA, LICHTNECKERT, ROBERT, OKADA, RYUICHI, ITO, KEI, RODRIGUES, VERONICA, & REICHERT, HEINRICH. 2008. Drosophila olfactory local interneurons and projection neurons derive from a common neuroblast lineage specified by the empty spiracles gene. *Neural Develop*, **3**(1), 33.

DAVIS, RONALD L. 2004. Olfactory learning. *Neuron*, **44**(1), 31–48.

DEMMER, HEIKE, & KLOPPENBURG, PETER. 2009. Intrinsic membrane properties and inhibitory synaptic input of kenyon cells as mechanisms for sparse coding? *J Neurophysiol*, **102**(3), 1538–1550.

DING, Q., DONLY, B. C., TOBE, S. S., & BENDENA, W. G. 1995. Comparison of the allatostatin neuropeptide precursors in the distantly related cockroaches Periplaneta americana and Diploptera punctata. *Eur J Biochem*, **234**(3), 737–746.

DIRCKSEN, H., SKIEBE, P., ABEL, B., AGRICOLA, H., BUCHNER, K., MUREN, J. E., & NÄSSEL, D. R. 1999. Structure, distribution, and biological activity of novel members of the allatostatin family in the crayfish Orconectes limosus. *Peptides*, **20**(6), 695–712.

DISTLER, P. 1989. Histochemical demonstration of GABA-like immunoreactivity in cobalt labeled neuron individuals in the insect olfactory pathway. *Histochemistry*, **91**(3), 245–249.

DISTLER, P. 1990. Synaptic connections of dopamine-immunoreactive neurons in the antennal lobes of Periplaneta americana. Colocalization with GABA-like immunoreactivity. *Histochemistry*, **93**(4), 401–408.

DISTLER, P. G., GRUBER, C., & BOECKH, J. 1998. Synaptic connections between GABA-immunoreactive neurons and uniglomerular projection neurons within the antennal lobe of the cockroach, Periplaneta americana. *Synapse*, **29**(1), 1–13.

DISTLER, P.G., & BOECKH, J. 1997a. Synaptic connections between identified neuron types in the antennal lobe glomeruli of the cockroach, Periplaneta americana: I. Uniglomerular projection neurons. *J Comp Neurol*, **378**(3), 307–19.

DISTLER, P.G., & BOECKH, J. 1997b. Synaptik connections between identified neuron types in the antennal lobe glomeruli of the cockroach Periplaneta americana: II multiglomerular interneurons. *The Journal of Comparative Neurology*, **383**(4), 529–540.

DUVE, H., EAST, P. D., & THORPE, A. 1999. Regulation of lepidopteran foregut movement by allatostatins and allatotropin from the frontal ganglion. *J Comp Neurol*, **413**(3), 405–416.

EAST, P. D., THORPE, A., & DUVE, H. 1995. Leu-callatostatin gene expression in the blowflies Calliphora vomitoria and Lucilia cuprina studied by in situ

hybridisation: comparison with Leu-callatostatin confocal laser scanning immunocytochemistry. *Cell Tissue Res*, **280**(2), 355–364.

EISTHEN, HEATHER L. 2002. Why are olfactory systems of different animals so similar? *Brain Behav Evol*, **59**(5-6), 273–293.

ERNST, K. D., & BOECKH, J. 1983. A neuroanatomical study on the organization of the central antennal pathways in insects. III. Neuroanatomical characterization of physiologically defined response types of deutocerebral neurons in Periplaneta americana. *Cell Tissue Res*, **229**(1), 1–22.

ERNST, K. D., BOECKH, J., & BOECKH, V. 1977. A neuroanatomical study on the organization of the central antennal pathways in insects. *Cell Tissue Res*, **176**(3), 285–306.

EVERS, J. F., SCHMITT, S., SIBILA, M., & DUCH, C. 2005. Progress in functional neuroanatomy: precise automatic geometric reconstruction of neuronal morphology from confocal image stacks. *J Neurophysiol*, **93**(4), 2331–2342.

FIALA, ANDRÉ. 2007. Olfaction and olfactory learning in Drosophila: recent progress. *Curr Opin Neurobiol*, **17**(6), 720–726.

GALIZIA, C. GIOVANNI, & RÖSSLER, WOLFGANG. 2010. Parallel olfactory systems in insects: anatomy and function. *Annu Rev Entomol*, **55**, 399–420.

GAO, Q., YUAN, B., & CHESS, A. 2000. Convergent projections of Drosophila olfactory neurons to specific glomeruli in the antennal lobe. *Nat Neurosci*, **3**(8), 780–785.

GORCZYCA, M. G., & HALL, J. C. 1987. Immunohistochemical localization of choline acetyltransferase during development and in Chats mutants of Drosophila melanogaster. *J Neurosci*, **7**(5), 1361–1369.

HAMILL, O. P., MARTY, A., NEHER, E., SAKMANN, B., & SIGWORTH, F. J. 1981. Improved patch-clamp techniques for high-resolution current recording from cells and cell-free membrane patches. *Pflugers Arch*, **391**(2), 85–100.

HILDEBRAND, J. G., & SHEPHERD, G. M. 1997. Mechanisms of olfactory discrimination: converging evidence for common principles across phyla. *Ann Rev Neurosci*, **20**, 595–631. Times Cited: 242 Review English Cited References Count: 257 Wl507.

HOMBERG, U. MÜLLER, M. 1999a. *Insect olfaction*. Springer. Chap. Neuroactive Substances in the antennal lobe, pages 181–206.

HOMBERG, U. 1994. *Distribution of neurotransmitters in the insect brain*. Gustav Fischer Verlag, Stuttgart, Jena, New York.

HOMBERG, U. 2002. Neurotransmitters and neuropeptides in the brain of the locust. *Microsc Res Tech*, **56**(3), 189–209.

HOMBERG, U., HOSKINS, S. G., & HILDEBRAND, J. G. 1995. Distribution of acetylcholinesterase activity in the deutocerebrum of the sphinx moth Manduca sexta. *Cell Tissue Res*, **279**(2), 249–59.

HOMBERG, U. MÜLLER, U. 1999b. *Insect Olfaction*. Springer. Chap. Neuroactive substances in the antennal lobe., pages 181–206.

HOMBERG, UWE, BRANDL, CHRISTIAN, CLYNEN, ELKE, SCHOOFS, LILIANE, & VEENSTRA, JAN A. 2004. Mas-allatotropin/Lom-AG-myotropin I immunostaining in the brain of the locust, Schistocerca gregaria. *Cell Tissue Res*, **318**(2), 439–457.

HORODYSKI, FRANK M., VERLINDEN, HELEEN, FILKIN, NANDA, VANDERSMISSEN, HANS PETER, FLEURY, CHRISTOPHE, REYNOLDS, STUART E., KAI, ZHEN-PENG, & BROECK, JOZEF VANDEN. 2011. Isolation and functional characterization of an allatotropin receptor from Manduca sexta. *Insect Biochem Mol Biol*, **41**(10), 804–814.

HOSKINS, S. G., HOMBERG, U., KINGAN, T. G., CHRISTENSEN, T. A., & HILDEBRAND, J. G. 1986. Immunocytochemistry of GABA in the antennal lobes of the sphinx moth Manduca sexta. *Cell Tissue Res*, **244**(2), 243–52.

HUANG, JU, ZHANG, WEI, QIAO, WENHUI, HU, AIQUN, & WANG, ZUOREN. 2010. Functional connectivity and selective odor responses of excitatory local interneurons in Drosophila antennal lobe. *Neuron*, **67**(6), 1021–1033.

HUSCH, ANDREAS, PAEHLER, MORITZ, FUSCA, DEBORA, PAEGER, LARS, & KLOPPENBURG, PETER. 2009a. Calcium current diversity in physiologically different local interneuron types of the antennal lobe. *J Neurosci*, **29**(3), 716–726.

HUSCH, ANDREAS, PAEHLER, MORITZ, FUSCA, DEBORA, PAEGER, LARS, & KLOPPENBURG, PETER. 2009b. Distinct electrophysiological properties in subtypes of nonspiking olfactory local interneurons correlate with their cell type-specific Ca2+ current profiles. *J Neurophysiol*, **102**(5), 2834–2845.

IGNELL, R. 2001. Monoamines and neuropeptides in antennal lobe interneurons of the desert locust, Schistocerca gregana: an immunocytochemical study. *Cell Tissue Res.*, **306**(1), 143–56.

IGNELL, RICKARD, ROOT, CORY M, BIRSE, RYAN T, WANG, JING W, NÄSSEL, DICK R, & WINTHER, ASA M E. 2009. Presynaptic peptidergic modulation of olfactory receptor neurons in Drosophila. *Proc Natl Acad Sci U S A*, **106**(31), 13070–13075.

ITOH, N., SLEMMON, J. R., HAWKE, D. H., WILLIAMSON, R., MORITA, E., ITAKURA, K., ROBERTS, E., SHIVELY, J. E., CRAWFORD, G. D., & SALVATERRA, P. M. 1986. Cloning of Drosophila choline acetyltransferase cDNA. *Proc Natl Acad Sci U S A*, **83**(11), 4081–4085.

KANZAKI, R., ARBAS, E. A., STRAUSFELD, N. J., & HILDEBRAND, J. G. 1989. Physiology and morphology of projection neurons in the antennal lobe of the male moth Manduca sexta. *J Comp Physiol A*, **165**(4), 427–453.

KARHUNEN, T., VILIM, F. S., ALEXEEVA, V., WEISS, K. R., & CHURCH, P. J. 2001. Targeting of peptidergic vesicles in cotransmitting terminals. *J Neurosci*, **21**(3), RC127.

KITAMOTO, T., IKEDA, K., & SALVATERRA, P. M. 1992. Analysis of cis-regulatory elements in the 5′ flanking region of the Drosophila melanogaster choline acetyltransferase gene. *J Neurosci*, **12**(5), 1628–1639.

KOLODZIEJCZYK, AGATA, SUN, XUEJUN, MEINERTZHAGEN, IAN A., & NÄSSEL, DICK R. 2008. Glutamate, GABA and acetylcholine signaling components in the lamina of the Drosophila visual system. *PLoS One*, **3**(5), e2110.

KREISSL, S., & BICKER, G. 1989. Histochemistry of acetylcholinesterase and immunocytochemistry of an acetylcholine receptor-like antigen in the brain of the honeybee. *J Comp Neurol*, **286**(1), 71–84.

KREISSL, SABINE, STRASSER, CHRISTINE, & GALIZIA, C. GIOVANNI. 2010. Allatostatin immunoreactivity in the honeybee brain. *J Comp Neurol*, **518**(9), 1391–1417.

KÖNNER, A CHRISTINE, HESS, SIMON, TOVAR, SULAY, MESAROS, ANDREA, SÁNCHEZ-LASHERAS, CARMEN, EVERS, NADINE, VERHAGEN, LINDA A W., BRÖNNEKE, HELLA S., KLEINRIDDERS, ANDRÉ, HAMPEL, BRIGITTE, KLOPPENBURG, PETER, & BRÜNING, JENS C. 2011. Role for insulin signaling in catecholaminergic neurons in control of energy homeostasis. *Cell Metab*, **13**(6), 720–728.

LAEMMLI, U. K. 1970. Cleavage of structural proteins during the assembly of the head of bacteriophage T4. *Nature*, **227**(5259), 680–685.

LAI, SEN-LIN, AWASAKI, TAKESHI, ITO, KEI, & LEE, TZUMIN. 2008. Clonal analysis of Drosophila antennal lobe neurons: diverse neuronal architectures in the lateral neuroblast lineage. *Development*, **135**(17), 2883–2893.

LAURENT, G. 1999. A systems perspective on early olfactory coding. *Science*, **286**(5440), 723–728.

LEMON, W. C., & GETZ, W. M. 1998. Responses of cockroach antennal lobe projection neurons to pulsatile olfactory stimuli. *Ann N Y Acad Sci*, **855**(Nov), 517–520.

LEMON, W. C., & GETZ, W. M. 2000. Rate code input produces temporal code output from cockroach antennal lobes. *Biosystems*, **58**(1-3), 151–158.

LOESEL, R., & HOMBERG, U. 1999. Histamine-immunoreactive neurons in the brain of the cockroach Leucophaea maderae. *Brain Res*, **842**(2), 408–18.

LUNDQUIST, C. T., & NÄSSEL, D. R. 1997. Peptidergic activation of locust dorsal unpaired median neurons: depolarization induced by locustatachykinins may be mediated by cyclic AMP. *J Neurobiol*, **33**(3), 297–315.

MAESTRO, J. L., BELLÉS, X., PIULACHS, M. D., THORPE, A., & DUVE, H. 1998. Localization of allatostatin-immunoreactive material in the central nervous system, stomatogastric nervous system, and gut of the cockroach Blattella germanica. *Arch Insect Biochem Physiol*, **37**(4), 269–282.

MALUN, D. 1991a. Inventory and distribution of synapses of identified uniglomerular projection neurons in the antennal lobe of Periplaneta americana. *J Comp Neurol*, **305**(2), 348–60. 0021-9967 Journal Article.

MALUN, D. 1991b. Synaptic relationships between GABA-immunoreactive neurons and an identified uniglomerular projection neuron in the antennal lobe of Periplaneta americana: a double-labeling electron microscopic study. *Histochemistry*, **96**(3), 197–207.

MALUN, D., WALDOW, U., KRAUS, D., & BOECKH, J. 1993. Connections between the deutocerebrum and the protocerebrum, and neuroanatomy of several classes of deutocerebral projection neurons in the brain of male Periplaneta americana. *J Comp Neurol*, **329**(2), 143–62. 0021-9967 Journal Article.

MANDERS, E. M. M., VERBEEK, F. J., & ATEN, J. A. 1993. Measurement of Colocalization of Objects In Dual-color Confocal Images. *Journal of Microscopy-oxford*, **169**, 375–382.

MERIGHI, A. 2002. Costorage and coexistence of neuropeptides in the mammalian CNS. *Prog Neurobiol*, **66**(3), 161–190.

NASSEL, D. R., & HOMBERG, U. 2006. Neuropeptides in interneurons of the insect brain. *Cell and Tissue Research*, **326**(1), 1–24.

NEHER, E. 1992. Correction for liquid junction potentials in patch clamp experiments. *Methods Enzymol*, **207**, 123–131.

NEUPERT, SUSANNE, SCHATTSCHNEIDER, SEBASTIAN, & PREDEL, REINHARD. 2009. Allatotropin-related peptide in cockroaches: identification via mass spectrometric analysis of single identified neurons. *Peptides*, **30**(3), 489–494.

NEUPERT, SUSANNE, FUSCA, DEBORA, SCHACHTNER, JOACHIM, KLOPPENBURG, PETER, & PREDEL, REINHARD. 2012. Toward a single-cell-based analysis of neuropeptide expression in Periplaneta americana antennal lobe neurons. *J Comp Neurol*, **520**(4), 694–716.

NISHINO, HIROSHI, YAMASHITA, SHINGO, YAMAZAKI, YOSHIYUKI, NISHIKAWA, MICHIKO, YOKOHARI, FUMIO, & MIZUNAMI, MAKOTO. 2003. Projection neurons originating from thermo- and hygrosensory glomeruli in the antennal lobe of the cockroach. *J Comp Neurol*, **455**(1), 40–55.

NÄSSEL, D. R. 1999. Tachykinin-related peptides in invertebrates: a review. *Peptides*, **20**(1), 141–158.

NÄSSEL, D. R., PERSSON, M. G., & MUREN, J. E. 2000. Baratin, a nonamidated neurostimulating neuropeptide, isolated from cockroach brain: distribution and actions in the cockroach and locust nervous systems. *J Comp Neurol*, **422**(2), 267–286.

NÄSSEL, DICK R, & WINTHER, ASA M E. 2010. Drosophila neuropeptides in regulation of physiology and behavior. *Prog Neurobiol*, **92**(1), 42–104.

OLSEN, SHAWN R, & WILSON, RACHEL I. 2008. Lateral presynaptic inhibition mediates gain control in an olfactory circuit. *Nature*, **452**(7190), 956–960.

OLSEN, SHAWN R, BHANDAWAT, VIKAS, & WILSON, RACHEL I. 2007. Excitatory interactions between olfactory processing channels in the Drosophila antennal lobe. *Neuron*, **54**(1), 89–103.

OTSUKA, M., & YOSHIOKA, K. 1993. Neurotransmitter functions of mammalian tachykinins. *Physiol Rev*, **73**(2), 229–308.

PREDEL, R., RAPUS, J., & ECKERT, M. 2001. Myoinhibitory neuropeptides in the American cockroach. *Peptides*, **22**(2), 199–208.

PREDEL, REINHARD, NEUPERT, SUSANNE, ROTH, STEFFEN, DERST, CHRISTIAN, & NÄSSEL, DICK R. 2005. Tachykinin-related peptide precursors in two cockroach species. *FEBS J*, **272**(13), 3365–3375.

REICHWALD, K., UNNITHAN, G. C., DAVIS, N. T., AGRICOLA, H., & FEYEREISEN, R. 1994. Expression of the allatostatin gene in endocrine cells of the cockroach midgut. *Proc Natl Acad Sci U S A*, **91**(25), 11894–11898.

ROOT, CORY M., SEMMELHACK, JULIA L., WONG, ALLAN M., FLORES, JORGE, & WANG, JING W. 2007. Propagation of olfactory information in Drosophila. *Proc Natl Acad Sci U S A*, **104**(28), 11826–11831.

RUDWALL, A. J., SLIWOWSKA, J., & NÄSSEL, D. R. 2000. Allatotropin-like neuropeptide in the cockroach abdominal nervous system: myotropic actions, sexually dimorphic distribution and colocalization with serotonin. *J Comp Neurol*, **428**(1), 159–173.

RÖSSLER, WOLFGANG, & ZUBE, CHRISTINA. 2011. Dual olfactory pathway in Hymenoptera: evolutionary insights from comparative studies. *Arthropod Struct Dev*, **40**(4), 349–357.

SACHSE, S., & GALIZIA, CG. 2002. Role of inhibition for temporal and spatial odor representation in olfactory output neurons: a calcium imaging study. *J Neurophysiol.*, **87**(2), 1106–17.

SACHSE, SILKE, PEELE, PHILIPP, SILBERING, ANA F, GÜHMANN, MARTIN, & GALIZIA, C. GIOVANNI. 2006. Role of histamine as a putative inhibitory transmitter in the honeybee antennal lobe. *Front Zool*, **3**, 22.

SALIO, CHIARA, LOSSI, LAURA, FERRINI, FRANCESCO, & MERIGHI, ADALBERTO. 2006. Neuropeptides as synaptic transmitters. *Cell Tissue Res*, **326**(2), 583–598.

SALVATERRA, P. M., & MCCAMAN, R. E. 1985. Choline acetyltransferase and acetylcholine levels in Drosophila melanogaster: a study using two temperature-sensitive mutants. *J Neurosci*, **5**(4), 903–910.

SCHACHTNER, J., SCHMIDT, M., & HOMBERG, U. 2005. Organization and evolutionary trends of primary olfactory brain centers in Tetraconata (Crustacea plus Hexapoda). *Arthropod Structure & Development*, **34**(3), 257–299.

SCHEIDLER, ANGELIKA, KAULEN, PETER, BRU¨NING, GEROLD, & ERBER, JOACHIM. 1990. Quantitative autoradiographic localization of [125I][alpha]-bungarotoxin binding sites in the honeybee brain. *Brain Research*, **534**(1-2), 332 – 335.

SEKI, YOICHI, & KANZAKI, RYOHEI. 2008. Comprehensive morphological identification and GABA immunocytochemistry of antennal lobe local interneurons in Bombyx mori. *J Comp Neurol*, **506**(1), 93–107.

SEKI, YOICHI, RYBAK, JÜRGEN, WICHER, DIETER, SACHSE, SILKE, & HANSSON, BILL S. 2010. Physiological and morphological characterization of local interneurons in the Drosophila antennal lobe. *J Neurophysiol*, **104**(2), 1007–1019.

SHANG, YUHUA, CLARIDGE-CHANG, ADAM, SJULSON, LUCAS, PYPAERT, MARC, & MIESENBOCK, GERO. 2007. Excitatory Local Circuits and Their Implications for Olfactory Processing in the Fly Antennal Lobe. *Cell*, **128**(3), 601–612.

SILBERING, ANA F., & GALIZIA, C GIOVANNI. 2007. Processing of odor mixtures in the Drosophila antennal lobe reveals both global inhibition and glomerulus-specific interactions. *J Neurosci*, **27**(44), 11966–11977.

SILBERING, ANA F, OKADA, RYUICHI, ITO, KEI, & GALIZIA, C. GIOVANNI. 2008. Olfactory information processing in the Drosophila antennal lobe: anything goes? *J Neurosci*, **28**(49), 13075–13087.

SLEMMON, J. R., SALVATERRA, P. M., CRAWFORD, G. D., & ROBERTS, E. 1982. Purification of choline acetyltransferase from Drosophila melanogaster. *J Biol Chem*, **257**(7), 3847–3852.

SLEMMON, J. R., CAMPBELL, G. A., SELSKI, D. J., & BRAMSON, H. N. 1991. The amino terminus of the putative Drosophila choline acetyltransferase precursor is cleaved to yield the 67 kDa enzyme. *Brain Res Mol Brain Res*, **9**(3), 245–252.

STOPFER, M., BHAGAVAN, S., SMITH, B. H., & LAURENT, G. 1997. Impaired odour discrimination on desynchronization of odour-encoding neural assemblies. *Nature*, **390**(6655), 70–74.

STOPFER, MARK. 2005. Olfactory coding: inhibition reshapes odor responses. *Curr Biol*, **15**(24), R996–R998.

STRAUSFELD, N. J., & HILDEBRAND, J. G. 1999. Olfactory systems: common design, uncommon origins? *Curr Opin Neurobiol*, **9**(5), 634–639. Times Cited: 22 Article English Cited References Count: 71 248fv.

SUGIHARA, H., ANDRISANI, V., & SALVATERRA, P. M. 1990. Drosophila choline acetyltransferase uses a non-AUG initiation codon and full length RNA is inefficiently translated. *J Biol Chem*, **265**(35), 21714–21719.

TAKAGAWA, K., & SALVATERRA, P. 1996. Analysis of choline acetyltransferase protein in temperature sensitive mutant flies using newly generated monoclonal antibody. *Neurosci Res*, **24**(3), 237–243.

TANAKA, NOBUAKI K, ITO, KEI, & STOPFER, MARK. 2009. Odor-evoked neural oscillations in Drosophila are mediated by widely branching interneurons. *J Neurosci*, **29**(26), 8595–8603.

UTZ, SANDRA, & SCHACHTNER, JOACHIM. 2005. Development of A-type allatostatin immunoreactivity in antennal lobe neurons of the sphinx moth Manduca sexta. *Cell Tissue Res*, **320**(1), 149–162.

UTZ, SANDRA, HUETTEROTH, WOLF, WEGENER, CHRISTIAN, KAHNT, JÖRG, PREDEL, REINHARD, & SCHACHTNER, JOACHIM. 2007. Direct peptide profiling of lateral cell groups of the antennal lobes of Manduca sexta reveals specific composition and changes in neuropeptide expression during development. *Dev Neurobiol*, **67**(6), 764–777.

UTZ, SANDRA, HUETTEROTH, WOLF, VÖMEL, MATTHIAS, & SCHACHTNER, JOACHIM. 2008. Mas-allatotropin in the developing antennal lobe of the sphinx moth Manduca sexta: distribution, time course, developmental regulation, and colocalization with other neuropeptides. *Dev Neurobiol*, **68**(1), 123–142.

VAN LOY, TOM, VANDERSMISSEN, HANS PETER, POELS, JEROEN, VAN HIEL, MATTHIAS B., VERLINDEN, HELEEN, & VANDEN BROECK, JOZEF. 2010. Tachykinin-related peptides and their receptors in invertebrates: a current view. *Peptides*, **31**(3), 520–524.

VANDEN BROECK, J., TORFS, H., POELS, J., VAN POYER, W., SWINNEN, E., FERKET, K., & DE LOOF, A. 1999. Tachykinin-like peptides and their receptors. A review. *Ann N Y Acad Sci*, **897**, 374–387.

VEENSTRA, J. A., LAU, G. W., AGRICOLA, H. J., & PETZEL, D. H. 1995. Immunohistological localization of regulatory peptides in the midgut of the female mosquito Aedes aegypti. *Histochem Cell Biol*, **104**(5), 337–347.

VEENSTRA, JAN A., & HAGEDORN, HENRY H. 1993. Sensitive enzyme immunoassay for Manduca allatotropin and the existence of an allatotropin-immunoreactive peptide in Periplaneta americana. *Archives of Insect Biochemistry and Physiology*, **23**(3), 99–109.

VITZTHUM, H., HOMBERG, U., & AGRICOLA, H. 1996. Distribution of Dip-allatostatin I-like immunoreactivity in the brain of the locust Schistocerca gregaria with detailed analysis of immunostaining in the central complex. *J Comp Neurol*, **369**(3), 419–437.

VOSSHALL, LESLIE B, & STOCKER, REINHARD F. 2007. Molecular architecture of smell and taste in Drosophila. *Annu Rev Neurosci*, **30**, 505–533.

WALDROP, B., CHRISTENSEN, T. A., & HILDEBRAND, J. G. 1987. GABA-mediated synaptic inhibition of projection neurons in the antennal lobes of the sphinx moth, Manduca sexta. *J Comp Physiol [A]*, **161**(1), 23–32.

WILSON, R. I., & LAURENT, G. 2005. Role of GABAergic inhibition in shaping odor-evoked spatiotemporal patterns in the Drosophila antennal lobe. *J Neurosci*, **25**(40), 9069–79.

WILSON, RACHEL I. 2008. Neural and behavioral mechanisms of olfactory perception. *Curr Opin Neurobiol*, **18**(4), 408–412.

WILSON, RACHEL I, & MAINEN, ZACHARY F. 2006. Early events in olfactory processing. *Annu Rev Neurosci*, **29**, 163–201.

WILSON, RACHEL I, TURNER, GLENN C, & LAURENT, GILLES. 2004. Transformation of olfactory representations in the Drosophila antennal lobe. *Science*, **303**(5656), 366–370.

WINTHER, ASA M E, & IGNELL, RICKARD. 2010. Local peptidergic signaling in the antennal lobe shapes olfactory behavior. *Fly (Austin)*, **4**(2), 167–171.

YASUYAMA, K., KITAMOTO, T., & SALVATERRA, P. M. 1995. Immunocytochemical study of choline acetyltransferase in Drosophila melanogaster: an analysis of cis-regulatory regions controlling expression in the brain of cDNA-transformed flies. *J Comp Neurol*, **361**(1), 25–37.

YASUYAMA, KOUJI, MEINERTZHAGEN, IAN A, & SCHÜRMANN, FRIEDRICH-WILHELM. 2003. Synaptic connections of cholinergic antennal lobe relay neurons innervating the lateral horn neuropile in the brain of Drosophila melanogaster. *J Comp Neurol*, **466**(3), 299–315.

Erklärung

Ich versichere, dass ich die von mir vorgelegte Dissertation selbständig angefertigt, die benutzten Quellen und Hilfsmittel vollständig angegeben und die Stellen der Arbeit – einschlie§lich Tabellen, Karten und Abbildungen –, die anderen Werken im Wortlaut oder dem Sinn nach entnommen sind, in jedem Einzelfall als Entlehnung kenntlich gemacht habe; dass diese Dissertation noch keiner anderen Fakultät oder Universität zur Prüfung vorgelegen hat; dass sie – abgesehen von unten angegebenen Teilpublikationen – noch nicht veröffentlicht worden ist sowie, dass ich eine solche Veröffentlichung vor Abschluss des Promotionsverfahrens nicht vornehmen werde.

Die Bestimmungen der Promotionsordnung sind mir bekannt. Die von mir vorgelegte Dissertation ist von Prof. Dr. Peter Kloppenburg betreut worden.

Köln, den 26.09.2012

(Debora Fuscà)

Teilpublikationen

Artikel

HUSCH, A, PAEHLER, M, FUSCA, D, PAEGER, L, KLOPPENBURG, CALCIUM CURRENT DIVERSITY IN PHYSIOLOGICALLY DIFFERENT LOCAL INTERNEURON TYPES OF THE ANTENNAL LOBE. *J. Neurosci.*, **29**(3), 716–726.

HUSCH, A, PAEHLER, M, FUSCA, D, PAEGER, L, KLOPPENBURG, P. 2009. DISTINCT ELECTROPHYSIOLOGICAL PROPERTIES IN SUBTYPES OF NONSPIKING OLFACTORY LOCAL INTERNEURONS CORRELATE WITH THEIR CELL TYPE-SPECIFIC CA2+ CURRENT PROFILES. *J. Neurophysiol.*, **102**, 2834–2845.

NEUPERT, S, FUSCA, D, SCHACHTNER, J, KLOPPENBURG, P, PREDEL, R. 2012. TOWARD A SINGLE-CELL-BASED ANALYSIS OF NEUROPEPTIDE EXPRESSION IN PERIPLANETA AMERICANA ANTENNAL LOBE NEURONS. *J. Comp. Neurol.*, **520**, 694–716.

FUSCA, D*, NEUPERT, S*, PAEGER, L., KERSTING, A., KLOPPENBURG, P, PREDEL, R. 2012. REPORTS ON SINGLE CELL LEVEL BASED ON 'OMICS'-TECHNOLOGIES AND PERFORATED PATCH RECORDINGS. (IN PREPARATION)

FUSCA, D, HUSCH, A, BAUMANN, A, KLOPPENBURG P.. 2012 CHOLINE ACETYLTRANSFERASE-LIKE IMMUNOREACTIVITY IN A PHYSIOLOGICALLY DISTINCT SUBTYPE OF NON-SPIKING LOCAL INTERNEURONS OF THE ANTENNAL LOBE. (IN PREPARATION)

FUSCA, D, NEUPERT, S, SCHACHTNER, J, PREDEL, R, KLOPPENBURG, P. 2012. NEUROPEPTIDES IN THE ANTENNAL LOBE. A STUDY ON IDENTIFIED LOCAL INTERNEURONS. (IN PREPARATION)

Poster

DEMMER, H, FUSCA, D, KLOPPENBURG, P. 2007. PHYSIOLOGICAL PROPERTIES OF KENYON CELLS RECORDED IN AN INTACT BRAIN PREPARATION. *Proceedings of the 31th Göttingen Neurobiology Conference and the 7th Meeting of the German Neuroscience Society.*

FUSCA, D, HUSCH, A, KLOPPENBURG, P. 2009. PHYSIOLOGICAL AND MORPHOLOGICAL FEATURES OF LOCAL INTERNEURONS IN THE ANTENNAL LOBE OF *Periplaneta americana*. *Proceedings of the 32th Göttingen Neurobiology Conference and the 8th Meeting of the German Neuroscience Society.*

FUSCA, D, NEUPERT, S, SCHACHTNER, J, PREDEL, R, KLOPPENBURG, P. 2011. NEUROPEPTIDES OF IDENTIFIED LOCAL INTERNEURONS IN THE ANTENNAL LOBE OF *Periplaneta americana*. *Proceedings of the 33th Göttingen Neurobiology Conference and the 9th Meeting of the German Neuroscience Society.*

Vorträge

FUSCA, D, NEUPERT, S, SCHACHTNER, J, PREDEL, R, KLOPPENBURG, P. 2011. PEPTIDE INVENTORY OF IDENTIFIED LOCAL INTERNEURONS IN THE ANTENNAL LOBE OF *Periplaneta americana*. *12th ESITO (European Symposium for Insect Taste and Olfaction) St.-Petersburg, Russian Federation, 6, p 6.*